Articles in PresS. J Neurophysiol (October 19, 2016). doi:10.1152/jn.00628.2016

Rhythm generation, coordination, and initiation in the vocal pathways of male African clawed frogs

Ayako Yamaguchi, Jessica Cavin Barnes, and Todd Appleby

Department of Biology, University of Utah,

257 South 1400 East, Salt Lake City, UT 84112-0840

Running head: Basic architecture of vocal CPG in *Xenopus laevis (42 chars)*

Corresponding author: Ayako Yamaguchi

Department of Biology

University of Utah

257 South 1400 East,

Salt Lake City, UT 84112-0840

a.yamaguchi@utah.edu

Number of figures: 8

Number of tables: 0

Abstract

Central pattern generators (CPG) in the brainstem are considered to underlie vocalizations in many vertebrate species, but the detailed mechanisms underlying how motor rhythms are generated, coordinated, and initiated remain unclear. We addressed these issues using isolated brain preparations of *Xenopus laevis* from which fictive vocalizations can be elicited. Advertisement calls of male *X. laevis* that consist of fast and slow trills are generated by vocal CPGs contained in the brainstem. Brainstem central vocal pathways consist of a premotor nucleus (DTAM) and a laryngeal motor nucleus (n.IX-X) with extensive reciprocal connections between the nuclei. In addition, DTAM receives descending inputs from the extended amygdala. We found that unilateral transection of the projections between DTAM and n.IX-X eliminated premotor fictive fast trill patterns but did not affect fictive slow trills, suggesting that the fast and slow trill CPGs are distinct; the slow trill CPG is contained in n.IX-X and the fast trill CPG spans DTAM and n.IX-X. Midline transections that eliminated the anterior, the posterior, or both commissures caused no change in the temporal structure of fictive calls, but bilateral synchrony was lost, indicating that the vocal CPGs are contained in the lateral halves of the brainstem and that the commissures synchronize the two oscillators. Furthermore, eliminating the inputs from extended amygdala to DTAM in addition to the anterior commissure resulted in autonomous initiation of fictive fast, but not slow trills by each hemibrainstem, indicating that the extended amygdala provides a bilateral signal to initiate fast trills.

New & Noteworthy

Central pattern generators (CPG) are considered to underlie vocalizations in many vertebrate species, but the detail mechanisms underlying their functions remain unclear. We addressed this

question using an isolated brain preparation of African clawed frogs. We discovered that two vocal phases are mediated by anatomically distinct CPGs, that there are a pair of CPGs contained in left and right half of the brainstem, and that mechanisms underlying initiation of the two vocal phases are distinct.

Keywords

central pattern generator, vocalization, parabrachial area, hindbrain, bilateral coordination, motor programs

Introduction

Many rhythmic motor programs including locomotion, breathing, and chewing behavior are generated by central pattern generators (CPGs), neural circuits that can function without rhythmic descending inputs or afferent feedback (Grillner 2006; Marder and Bucher 2001; Marder and Calabrese 1996). To understand the functions of CPGs, it is critical to identify neuronal components that make up CPGs, how they are coordinated, and in the case of episodic behavior, how CPG activity is initiated. Much effort to understand mechanisms underlying CPG function has been aided by the use of fictive preparations, *in vitro* preparations from which patterned neuronal activity that underlies rhythmic motor programs can be elicited (Sweeney and Kelley 2014). For example, fictive swimming (Buchanan 2011; Fetcho and McLean 2010; Roberts et al. 2012), walking (Kiehn et al. 2010), breathing (Garcia et al. 2011), and chewing (Marder et al. 2005) preparations played critical roles in advancing understanding of the neural mechanisms of CPGs underlying these rhythmic behaviors.

Vocalizations produced by vertebrates are often rhythmic and are thought to be mediated by CPGs (Jurgens and Hage 2007). Vocal CPGs in many vertebrate species, including humans (i.e., non-verbal vocal utterance such as laughter), are considered to be located within the brainstem and thought to retain significant homology across species (Bass et al. 2008). The CPG underlying vocalizations in African clawed frogs (*Xenopus laevis*) presents an excellent model to understand the function of vocal CPGs.

Advertisement calls produced by male *X. laevis* to attract females consist of fast and slow trills, each of which contains a series of sound pulses that are repeated at ~60Hz and ~30Hz, respectively (Fig 1A). These calls are produced when laryngeal motoneurons fire at 60 and 30Hz (Yamaguchi and Kelley 2000), causing contraction of a pair of laryngeal muscles at that rate, which pull apart arytenoid discs to produce each sound pulse (Yager 1992). It is critical that the left and right laryngeal muscles are activated synchronously to generate a proper sound pulse. The central vocal pathways of *X. laevis* consist of two pairs of brainstem nuclei: n.IX-X, a homologue of nucleus ambiguus and retroambiguus (Albersheim-Carter et al. 2016) that contains laryngeal motoneurons projecting to the laryngeal muscles via the laryngeal nerve, and the premotor nucleus of the dorsal tegmental area of medulla (DTAM), a homologue of the parabrachial area, (Fig 1B) which does not include any lower motor or primary sensory neurons, and thus are not associated with cranial nerves. Anatomical studies have shown that there are extensive reciprocal connections among these nuclei (Fig 1B). In addition to these reciprocal connections within the brainstem, DTAM is reciprocally connected with the central amygdala in the extended amygdala (Hall et al. 2013; Moreno and Gonzalez 2005), Fig 1B).

Previously, we developed a fictive vocalization preparation *in vitro* (Rhodes et al. 2007), only one of a few fictive vocalizing preparations developed in vertebrates to date (Chagnaud et al.

2011). Application of serotonin (5-HT) to an isolated whole brain *in vitro* elicits fictive calls that can be recorded via laryngeal nerves. Here, using the fictive calling preparation of male *X. laevis*, we analyzed the contribution of the projections connecting distinct brainstem nuclei to the rhythm generation, bilateral coordination, and initiation of calls. We discovered that CPGs for fast and slow trills include anatomically distinct populations of neurons contained in each lateral half of the brainstem whose timing are synchronized by the anterior and posterior commissures, and that the initiation of fast trills appears to be mediated by a bilaterally synchronous signal provided by the extended amygdala to DTAM. Our results represent the first detailed analyses of these vocal CPGs, and reveal new details of the functional architecture that underlies vocal production in male *X. laevis*, highlighting the complementary nature of the neural circuits that insure bilateral synchrony in rhythm generation and subsequent call initiation.

Materials and Methods

Animals

Forty four adult male *Xenopus laevis* obtained from Nasco (Fort Atkinson, WI, average $\pm$ std weight = 42.98 $\pm$ 4.11g, length = 7.16 $\pm$ 0.35cm) were used for unilateral transverse transection (Fig 2A, n = 8), anterior and posterior commissures sagittal transection (Fig 3A, n = 3), anterior commissure sagittal transection (Fig 4A, n = 6), posterior commissure sagittal transection (Fig 5A, n = 5), descending inputs transverse and anterior commissure sagittal transection (Fig 6A, n = 4), and descending inputs transverse transection (Fig 7C, n = 6). All

procedures were approved by the Institutional Animal Care and Use Committee at the University of Utah, and complied with National Institutes of Health guidelines.

Isolated brain preparation and fictive vocal recordings

Fictive vocalizations were elicited from the isolated brains of sexually mature adult males. Animals were anaesthetized with subcutaneous injection (0.3mL 1.3%) of tricaine methanesulfonate (MS-222; Sigma), decapitated on ice, and brains were removed from the skulls in a dish containing cold saline (in mM: 96 NaCl, 20 $NaHCO_3$, 2 $CaCl_2$, 2KCl, 0.5 $MgCl_2$, 10 HEPES, and 11 glucose, pH 7.8) oxygenated with 99% O_2. Brains were then brought back to the room temperature (22°C) over the next hour, and then transferred to a recording chamber which was superfused with oxygenated saline at 100ml per hour at room temperature.

In these isolated brains, the laryngeal nerves are cut to about 7mm in length to be used for nerve recordings. Laryngeal nerve activity was recorded bilaterally using a suction electrode placed over cranial nerve (N.) IX-X. Local field potential (LFP) recordings from DTAM were obtained bilaterally using a 1 MΩ tungsten electrode (FHC, Bowdoin, ME). Fictive vocalizations were elicited by bath-application of 5-HT (Sigma) using a 1ml pipette. In response to 5-HT, a series of compound action potentials (CAPs) that are virtually identical to those recorded from awake calling frogs can be recorded from the laryngeal nerves of an isolated brain (Rhodes et al., 2007, compare nerve recordings of Fig 1A (bottom trace) and Fig 3B (middle two traces), for example). Prior to the application of 5-HT, superfusion of saline through the recording chamber was suspended and 1ml of concentrated 5-HT solution (0.6mM in dH_2O) was added to the 20ml bath (30μM, final concentration). Nerve and LFP signals were amplified

1000x using differential amplifiers (Models 1700 and 1800, respectively; A-M Systems, Carlsborg, WA), and band-pass filtered (10Hz – 5kHz and 0.1 – 5kHz, respectively). All signals were digitized at 10 kHz (Digidata 1440A; Molecular Devices, Sunnyvale, CA), and recorded on a PC using Clampex software (Molecular Devices). After 5 minutes of recording in the presence of 5-HT, superfusion was reinstated at the maximum rate (~10ml/minute) for 5 minutes to wash out the 5-HT, then at a slower rate (~125ml/hour) for one hour between 5-HT applications.

Transection of isolated brains

After fictive advertisement calls were recorded from intact brains, transections were made using a scalpel. Prior to transection, brains were placed on ice and brought to 4 ± 2°C. For unilateral transverse transection, a cut was made posterior to the VIIIth nerve from midline to the lateral edge of the brain on either left or right side of the brainstem (Fig 2A). For anterior commissure sagittal transection, a cut was made along the midline between the rostral optic tectum and trigeminal nerve (CN V) ventral to the ventricle (Fig 4A), severing all the projections between the two DTAMs. For posterior commissure sagittal transection a cut was made along the midline between an area 1mm rostral to the nerve IX-X and the obex ventral to the ventricle (Fig 5A), severing all the projections between the two n.IX-Xs. For descending inputs transverse transection, a cut was made at the level of the anterior optic tectum (Fig 7C), severing all the connection between extended amygdala and DTAM. In brains with anterior and posterior commissure sagittal transection, and those with anterior commissure sagittal and descending inputs transverse transection, both cuts were made in each brain (Fig 3A, 6A). After the

158 transection, the brains were placed in a holding dish containing oxygenated saline (200mL) and
159 gradually returned to the room temperature over the next hour before 5-HT was applied again.
160
161 *Analysis of in vitro* fictive *vocalizations*
162
163 To determine how transections affect the central vocal pathways, we examined the fictive
164 fast and slow trill rates, and the bilateral synchrony of the motor outputs produced. Ten bouts of
165 calling were selected at random for each animal before and after the transection. Compound
166 action potentials (CAPs) corresponding to laryngeal motoneuron activity were identified using
167 Clampfit (Molecular Devices, Sunnyvale, CA) using a threshold search function (threshold set at
168 3 standard deviation of background noise, minimum event duration of 0.4ms), and instantaneous
169 CAP rates were calculated based on inter-CAP peak interval. When a brain produces a series of
170 fictive advertisement calls, it is sometimes difficult to distinguish the end of fictive slow trills
171 and the beginning of the next fictive fast trill. In this case, we used DTAM activity to distinguish
172 the two types of fictive trills; CAPs accompanied by activity (or larger activity) in DTAM were
173 defined as a part of fictive fast trills and those without (or with smaller) DTAM activity were
174 considered to be a part of fictive slow trills (see Fig 3B, rectangle show transition from slow to
175 fast trills, for example). A frequency histogram of CAP rate during fictive fast and slow trills of
176 each animal before and after transection showed a normal distribution and were fit with Gaussian
177 curves with mean of μ for fictive fast and slow trills, which was used for statistical analyses.
178 The *Xenopus* larynx generates sound pulses when both laryngeal muscles are activated
179 simultaneously and pull apart a pair of arytenoid discs. Accordingly, the central vocal pathways
180 of intact *Xenopus* brains activate left and right laryngeal motoneurons nearly synchronously (see

Fig 3C, for example). To evaluate the synchronicity of the motor activity of the left and right side before and after the transection, cross correlation coefficients between the left and right nerve activity were calculated while sliding one nerve recording against the other across time (± 10msec, e.g., Fig 3F). To this end, left and right nerve recordings containing ten consecutive fictive fast and slow trill CAPs were used to calculate cross correlation coefficients. The time of the maximum cross correlation coefficients ("the peak lag time") was identified for fictive fast and slow trills before and after the transection for each animal. The peak lag time of zero indicates synchronous activity of the two nerves and deviation from zero indicates delay between the two nerves. We took the absolute value of the peak lag time ("absolute peak lag time") for statistical tests, since our goal in most analyses was to determine how much the peak deviated from zero. In cases where we suspected that CAPs on one nerve leads the other, we also took the absolute value of the peak lag time to demonstrate the time lag between the two nerves. For the double transection that involves transection between extended amygdala and DTAM and anterior commissure (Fig 6A), each CAP (instead of ten consecutive CAPs) was cross-correlated against the other to characterize moment-to-moment changes in the relative timing of CAPs on each side (Fig 6).

Statistical analyses

All statistical analyses were done using StatView software (SAS Institute, Cary, NC). For fictive trill rates, absolute peak lag time, and maximum CAP amplitude for fictive fast and slow trills, Wilcoxon signed-rank test was used to compare the value before and after the transection within individuals.

Results

Are fast and slow trills generated by the same neural elements?

Are the fast and slow trill generated by shared neural circuitry or by anatomically distinct neural networks? Our previous study shows that LFP recordings obtained from DTAM are active mostly during fast, but not during slow trills (see Fig 3B, 7A, for example), suggesting that fast trills but not slow trills are mediated by DTAM. To directly test this possibility, we transected the projections between DTAM and n.IX-X (Fig 2A) and examined the fictive advertisement calls elicited in response to 5-HT. Previously, we have shown that *bilaterally* transecting the projection between the DTAM and n.IX-X transversely abolishes 5-HT-induced fictive call production entirely (Rhodes et al. 2007). With the absence of fictive vocalizations, however, it was not possible to determine if the transection disrupts the mechanisms underlying vocal initiation or the rhythm generation. Here, we reasoned that *unilaterally* transecting the projection between n.IX-X and DTAM (unilateral transverse transection, Fig 2A) may spare the vocal initiation and provide us with an opportunity to examine the role of the n.IX-X to DTAM projection in fast and slow trill generation.

In striking contrast to the *bilateral* transverse transection, the unilaterally transected brains produced fictive advertisement calls in response to 5-HT (Fig 2B, n = 8). The rates of fictive fast and slow trill did not show any significant change after transection (Z = -0.980, -1.694, p = 0.327, 0.091 for fictive fast and slow trills, respectively, Fig 2C), indicating that CPGs remaining in the transected brains are capable of generating normal vocal rhythms. However, fictive advertisement calls produced by the unilaterally transected brains showed some abnormality that was detected *only* during fictive fast trills. The timing of the CAPs recorded

227 from the transected side significantly lagged behind those recorded from the intact side during
228 fictive fast trills, but not during fictive slow trills (Fig 2D). Accordingly, the cross correlation
229 peak for fictive fast trills was not centered near zero after the transection whereas the peak for
230 the fictive slow trill remained near zero (Fig 2E). Absolute peak lag time showed a significant
231 increase only for fictive fast trills after the transection ($Z = -2.380, -1.690$, $p = 0.0172, 0.091$ for
232 fictive fast and slow trills, respectively, Fig 2F). In addition, the maximum amplitude of the
233 CAPs recorded from the both nerves became significantly smaller after transection during fictive
234 fast trills ($Z = -2.521, -2.380$, $p = 0.012, 0.017$ for intact and transected sides, respectively, Fig
235 2G), but not during fictive slow trills ($Z = -0.676, -0.169$, $p = 0.499, 0.866$ for intact and
236 transected sides, respectively, Fig 2G). These results suggest that unilateral transection of the
237 projection between n.IX-X and DTAM selectively impacts fast trills.
238 We suspected that the fast trill CPGs on the transected side became dysfunctional after
239 transection, and the reason why the laryngeal motoneurons on the transected side generate any
240 CAPs at all during fictive fast trills was because they were driven by the functional CPG on the
241 contralateral intact side. To test this possibility, we examined local field potential (LFP)
242 recordings obtained from the left and right DTAMs of the transected brains. As described
243 previously (Zornik et al. 2010), DTAM local field potential recordings of intact brains contain
244 "waves" (baseline fluctuations) that coincide with onset and offset of the fictive fast trills, and
245 phasic activity riding on top of the waves (see Fig 3B, top and bottom traces, for example) that
246 peak at around 60Hz (Fig 2H left two graphs). In these transected brains, the LFP recordings
247 obtained from DTAM on the intact side after the transection were no different from those
248 obtained from intact brains, containing waves with phasic activity (Fig 2B top trace labeled as
249 left DTAM, intact side) with a peak frequency around 60Hz (Fig 2H, compare before (top left)

and after (top right) the transection). However, LFPs obtained from the transected side showed waves without phasic activity (Fig 2B bottom trace labeled as right DTAM), as evident in the loss of a peak in the power spectrum after the transection (Fig 2H, compare before (bottom left) and after (bottom right) the transection, black arrow). The LFP activity on the transected side resemble 5-HT induced activity obtained from DTAM of brains in which DTAM and n.IX-X are bilaterally transected (Zornik et al. 2010). The results indicate that in the absence of the unilateral projections between DTAM and n.IX-X, the premotor activity in DTAM associated with fictive fast trills loses its phasic component and fails to drive the laryngeal motoneurons on the ipsilateral side even though an indirect path from DTAM to ipsilateral n.IX-X (from DTAM to contralateral DTAM, contralateral n.IX-X to ipsilateral n.IX-X) is available. The laryngeal motoneurons on the transected side, instead, are likely driven by the fast trill CPG on the contralateral (intact) side. The fast trill inputs from the contralateral side to the transected side, however, appear insufficient to make up for the loss of excitatory drive from ipsilateral DTAM, which is known to provide direct, monosynaptic glutamatergic inputs to the motoneurons (Zornik 2007). Based on these results, we conclude the CPGs for fast and slow trills rely on anatomically distinct neuronal elements: the slow trill rhythm generator operates without the rostro-caudal projections between DTAM and n.IX-X whereas the fast trill rhythm generator critically relies on these projections.

Are commissural interneurons important for rhythm generation?

Many CPGs rely on a half-center oscillator that consists of two neurons (or two groups of neurons) that are reciprocally coupled to each other by inhibitory synapses (Moult et al. 2013; Sakurai et al. 2014; Satterlie 1985). Although the constituent neurons of the half-center

oscillator are not rhythmogenic themselves, the reciprocal coupling together with the cellular mechanisms (such as escape from inhibition by activating I_H, or release of inhibition due to synaptic depression) endows the neurons with the ability to fire rhythmically at a variety of phases including anti-phase and in-phase depending on the synaptic rise-time (Wang and Rinzel, 1992, 1993, Van Vreeswijk et al., 1994, White et al., 1998). Here, we examined whether anterior and/or posterior commissural interneurons in *Xenopus* brainstem are a part of reciprocal inhibitory network and constitute the core of the fast and/or slow rhythm generators. To test these possibilities, we transected anterior and posterior commissures in the sagittal plane (Fig 3A) and examined the fictive advertisement calls generated by the transected brains in response to 5-HT application. If the commissures are a part of the half-center oscillator, the transection of the anterior and/or posterior commissures should eliminate rhythmic activity.

When both anterior and posterior commissures of brains that generate fictive advertisement calls (Fig 3B) were transected (Fig 3A), fictive advertisement calls were still elicited in response to 5-HT (Fig 3D, H, n=3). However, the fictive calls recorded from the right and left nerves became asynchronous after transection (Fig 3D, E). In intact brains, fictive fast and slow trills are initiated simultaneously (Fig 3B), and the CAPs are synchronous both during fictive fast and slow trills (Fig 3C). Accordingly, the mean absolute peak lag time (see Methods) between the CAPs recorded from the two laryngeal nerves of the intact brains were very small: 0.20 ± 0.03 msec and 0.27 ± 0.05 msec for fictive fast and slow trills, respectively (Fig 3F). In the double transected brains, in contrast, the onset and offset of the fictive fast and slow trills was not synchronous (Fig 3D compared to 3B, but see below), with fictive calls and trills sometimes recorded only from one nerve and not from the other (Fig 3D, the first fictive advertisement call recorded on the right, but not on the left nerve, labeled with a bracket and a black arrows; Fig 3H,

296 the first two calls contained fictive slow trills only on the left nerve, and the last call contain
297 fictive slow trills only on the right nerve, labeled with arrows). Furthermore the CAPs recorded
298 from the two nerves during fictive fast and slow trills were entirely asynchronous; the number of
299 CAPs produced in a given amount of time were not the same between the two nerves, and the
300 delay between the CAPs recorded from the two nerves varied greatly from one instance to
301 another (Fig 3E). As a consequence, there was no obvious peak in the cross-correlation between
302 the two nerve CAPs (Fig 3F; note that there should be a peak in the cross-correlation if the
303 activity of one nerve lags behind that of the other nerve with a consistent delay), and the
304 maximum cross correlation coefficient was reduced from 0.94 and 0.85 for the fast and slow
305 trills of intact brains to 0.18 and 0.10 for the fast and slow trills of transected brains, respectively.
306 Due to the absence of a clear peak in the CAP cross-correlation, we were not able to obtain a
307 mean absolute peak lag time from these transected brains. These results are consistent with the
308 idea that the commissures are not necessary for rhythm generation, but that they function to
309 synchronize the motor outputs from the two nerves.
310 Next, to examine the capability of rhythm generation of the fast and slow trill CPGs in
311 the left and right brainstem in isolation, we analyzed the rates of the fictive fast and slow trills
312 produced by double-transected brains. Since the two sides of the brain produce independent
313 vocal motor programs, we analyzed the fictive fast and slow trill rates recorded from each nerve
314 separately. The results showed that, after double transection, fictive fast trill rates recorded from
315 the two nerves decreased ($Z=-2.201$, $p=0.028$), while fictive slow trill rates remain unchanged
316 ($Z=-0.405$, $p=0.686$, Fig 3G). Although the decrease of the fast trill rates was statistically
317 significant, fictive fast trill rates after transection remained within the normal range of fast trills

generated by intact brains (Fig 3G, dotted green lines). Thus, CPGs contained in the right and left halves of the brainstem are capable of generating basic fast and slow trill rhythms.

To explore the function of the isolated hemibrainstem further, we examined premotor activity obtained from the DTAMs of double-transected brains. These recordings showed activity containing waves and phasic activity, as in intact brains, but the activity accompanied the fictive fast trill recorded from the ipsilateral, but not from the contralateral nerve (Fig 3D, top and bottom traces), confirming that each side of the brainstem generates its own fictive fast trill rhythms independently. Thus, DTAM is capable of generating normal premotor activity in the absence of the two commissures. Together, these results suggest that (1) the left and right brainstem contains autonomous CPGs for fast and slow trills that can generate basic vocal rhythms even when they are surgically isolated from their contralateral counterparts, and (2) the commissures function to bilaterally synchronize the activity of the CPGs on the two sides of the brainstem.

Which commissures are important for bilateral coordination?

We next examined which of the commissures play a role in synchronizing the two separate CPGs on each side of the brainstem. To this end, we first transected the anterior commissure alone (Fig 4A). These transected brains readily produced fictive fast and slow trills (Fig 4B, n = 6), and both trill rates did not change significantly after transection ($Z = -0.314, -1.572$, $p = 0.753, 0.116$ for fictive fast and slow trills, respectively, Fig 4C). In addition, the CAPs recorded from the two nerves appeared synchronous (Fig 4D, E), and accordingly, the absolute peak lag time showed little change for fictive fast and slow trills ($Z = -0.943, -0.943$, p

= 0.345, 0.345 for fictive fast and slow trills, respectively, Fig 4F). Thus, the anterior commissure by itself is not necessary for synchronizing the timing of CAPs generated by the right and left CPGs. Instead, the projections remaining in the brainstem (solid arrows in Fig 4A) can synchronize the timing of fast and slow trill CAPs generated by the two sides of the brainstem.

When the posterior commissure was transected alone (Fig 5A), fictive fast and slow trills were readily produced in response to 5-HT (Fig 5B, n = 5), and fictive fast and slow trill rates did not change significantly after transection (Z = -1.352, -0.674, p = 0.176, 0.5, for fictive fast and slow trills, respectively, Fig 5C). The timing of CAPs recorded from the right and left sides, however, became less synchronous after transection during both fictive fast and slow trills (Fig 5D, E). The absolute peak lag time between the right and left CAPs increased, on average ($\pm$s.e.), by 1.27 $\pm$ 0.36 and 2.01 $\pm$ 0.72 msec during fictive fast and slow trills, respectively, and these increases were significant (Fig 5F; Z = -2.201, -2.023, p = 0.028, 0.043 for fictive fast and slow trills, respectively). These results suggest that the posterior commissure plays a role in coupling the CPGs contained in left and right brainstem. Some or all of the projection neurons that were eliminated in these brains (dotted arrows in Fig 5A) contribute to bilaterally synchronizing the CAPs, and the remaining projections (solid arrows in Fig 5A) are not sufficient to compensate for the loss.

Although the majority of the fictive slow trills recorded from the brains with transected posterior commissures consist of CAPs with a consistent delay between the two nerves as described above (Fig 5D), some fictive slow trills recorded from the right and left nerves of the transected brains appeared asynchronous. An example in Figure 5G shows fictive slow trills recorded from the right and left nerves of a brain with the posterior commissure transected. The

fictive slow trill recorded from the two nerves contained different numbers of CAPs (16 CAPs on the left nerve, 14 CAPs on the right nerve) that were repeated at rates that differ between the two nerves. This asynchrony between the two nerves was never observed during fictive fast trills, indicating that the posterior commissure plays a more important role for the bilateral synchronization of the slow trill CPG than of fast trill CPG. Taken together, neither of the single transections completely and consistently decoupled the CPGs on the two halves of the brainstem, indicating that the two commissures play complementary roles in bilaterally synchronizing the CPGs.

Do descending projections from extended amygdala to DTAM initiate fast trills from the two sides of the brainstem synchronously?

In *X. laevis*, the bed nucleus of the stria terminalis (BNST) has been shown to be involved in male vocalizations. BNST is known to project to the rostral raphe nucleus (Moreno et al. 2012), a nucleus that expresses 5-HT_{2C} receptors that mediate initiation of fictive advertisement calls (Yu and Yamaguchi 2010). Electrical stimulation of the BNST *in vitro* elicits fictive advertisement calls, and lesioning of BNST *in vivo* reduces the calling behavior (Hall et al. 2013). Previously, however, we showed that a brainstem isolated from the descending inputs by transversely transecting at the level of the rostral optic tectum can still produce fictive advertisement calls in response to 5-HT (Rhodes et al. 2007), suggesting that extended amygdala is not necessary for the initiation of the advertisement calls. To resolve this paradox, we explored the mechanisms underlying initiation of fictive fast trills.

Analyses of the fictive advertisement calls produced by the brains with sagittal transections of anterior and posterior commissures provided evidence that descending projections from the extended amygdala to DTAM may play a role in initiating advertisement calls from the two sides of the brainstem simultaneously. In these double transected brains, fictive calls were sometimes recorded only from one side and not from the other (Fig 3D, the first call only recorded from the right nerve, bracket with black arrow). However, the majority of the calls (93.8%) were initiated from both sides within a relatively short time window; after a fictive fast trill is initiated by one side of the brain, the other side initiated the fictive fast trills within 7.0 to 316.4msec in double transected brains (average delay = 95.0msec). Thus, most calls recorded from the right and left nerves showed extensive overlap with each other (e.g., Fig 3H) even though CAPs are not at all synchronous (Fig 3E). This observation suggests that in these double-transected brains, there is a bilaterally synchronous signal descending from the extended amygdala to right and left DTAM that allows the fictive fast trills to be initiated by both sides of the brainstem near-synchronously in response to 5-HT.

In another experiment, we fortuitously discovered that there are redundant mechanisms within the central vocal pathways of *X. laevis* to initiate synchronous fast trills from the left and right sides. In four brains, sagittal transection was made to sever the anterior commissure, and bilateral transverse transection was made at the level of rostral optic tectum to remove descending inputs from the external amygdala to DTAMs. Out of four double-transected brains, only two produced full fictive advertisement calls including both fast and slow trills, and the remaining two produced calls that include only fast trills. Thus, we focused on the initiation of fast trills using all four brains. In these double-transected brains, fictive fast trills were initiated from both nerves near simultaneously (Fig 6B, middle two traces labeled as left and right nerves).

However, the amplitude and timing of the CAPs recorded from the two nerves were abnormal. In these brains, fictive fast trill CAPs recorded from one nerve had a significantly larger amplitude than those of their contralateral counterpart. Which nerve had a larger CAP amplitude was not consistent and often alternated. For example, in Fig 6B, the CAP amplitude of the right nerve is larger than that of the left nerve during the first and third fictive fast trills, and smaller during the second and fourth fictive fast trills (middle two traces). Furthermore, when the timing of fictive fast trill CAPs recorded from the right and left nerves was examined, the side with the larger CAPs always preceded the side with the smaller CAP (Fig 6D, D1, E, E1). These results suggest that premotor activity of the fictive fast trills is generated only by one side (right or left) of the brainstem in these double-transected brains, and projects to the silent side to drive the motoneurons. To explore this possibility, we examined premotor activity in DTAM directly.

Strikingly, the LFP wave and phasic activity in DTAM were only observed when the ipsilateral nerve produced large-amplitude CAPs (Fig. 6B). DTAM was silent on the side producing the delayed, small-amplitude CAPs on the other side (Fig 6B arrows). This observation suggest that in these double transected brains, fictive fast trills are initiated and generated entirely by DTAM on one side (left or right) of the brainstem while the other side remains silent.

Moreover, we found that activity in the two DTAMs could overlap in time. For example, in Fig 6F, right DTAM becomes active first and generates fictive fast trills with a large CAP amplitude that precede the small CAPs recorded from the left nerve (Fig 6F, G). About 800msec later, the left DTAM becomes active while the right DTAM continues to be active. This simultaneous activity of right and left DTAM results in CAPs from the both nerves with variable amplitude and delay (Fig 6G, G1). After about 200msec of simultaneous DTAM activity, right

433 DTAM becomes silent, and left DTAM continues its activity for another ~200msec by itself
434 while larger amplitude CAPs with a slight lead relative to the right CAPs are recorded from the
435 left nerve (Fig 6G). This observation suggests that, in these double transected brains, the fictive
436 fast trill is initiated by each side independently without any temporal coordination between the
437 two sides. Thus, in these double-transected brains, we were able to initiate fast trills from either
438 side of the brainstem independently.
439 Interestingly, in these transected brains, we observed that fictive slow trills were initiated
440 simultaneously (Fig 6H), and that CAPs recorded from the two nerves were synchronous (Fig 6I,
441 I1). These results indicate that even though the fictive fast trills are initiated autonomously by
442 each side of the brainstem in these double-transected brains, initiation and generation of fictive
443 slow trills is unaffected, suggesting the mechanisms of trill initiation differ between the fast and
444 slow trill CPGs.
445 The results obtained from the double transected brains are in stark contrast to results
446 obtained from the brains with either one of the transection alone. In brains in which the
447 projection from extended amygdala to DTAM is transected (n=6, Fig 7C), fictive vocalizations
448 are readily elicited in response to 5-HT (Fig 7D) as we have described previously (Rhodes et al.
449 2007), and the premotor activity is also initiated simultaneously by the left and right DTAM (Fig
450 7E, arrows pointing to top and bottom traces), as in the case of intact brains (Fig 7B, black
451 arrows). This premotor activity in intact and transected brains resulted in the simultaneous onset
452 of fast trill CAPs from the two nerves (Fig 7B, E, a line with arrows on both ends pointing to
453 middle two traces). When the anterior commissure was transected, we found that the onset of
454 premotor activity that accompanies fictive fast trills (Fig 7G, I, K) was variable. Premotor
455 activity of the two DTAMs was sometimes initiated simultaneously (Fig 7H, arrows pointing to

top and bottom traces), but at other times the activity in one DTAM preceded the activity in the contralateral DTAM (Fig. 7J, L, arrows pointing to top and bottom traces) by as long as 500msec (e.g., Fig 7J). Asynchronous initiation of DTAM activity is unlikely to be due to the positioning of the extracellular electrode, because these distinct patterns of DTAM activity (such as Fig 7H, J, and L) were observed in many consecutive calls when the electrodes were stationary. Despite the variability in the initiation of DTAM activity in these transected brains, the first CAP of the fictive fast trill appears to be generated from both nerves simultaneously (Fig 7H, J, L, lines with arrows on both ends pointing to middle two traces), presumably because the laryngeal motoneurons of the silent side are driven by the premotor signal from the contralateral active side. Taken together, the loss of one of the two projections does not cause unilateral fictive fast trill initiation, even though the transection of anterior commissure alone sometimes introduced the delay in the initiation of DTAM activity. Thus, we suggest that these two projections play redundant roles in initiating fast trills from the two sides simultaneously, and removal of both of the projections is required to decouple fast trill initiation from the two sides.

Discussion

Our results reveal the basic architecture of the vocal CPG that regulate call rhythm generation, coordination, and initiation. Based on these results, we propose a model of the vocal pattern generator in male *Xenopus laevis* as discussed below (Fig 8).

Central pattern generators for fast and slow trills

In this study, we first examined if neural elements that make up the fast and slow CPGs are distinct. A male *Xenopus laevis* is known to change the duration of the fast and slow trills

479 depending on its state of arousal; when a male detects a sexually receptive females, the duration
480 of the fast trill is elongated while the duration of slow trills is shortened. It is conceivable that
481 the neural circuitry that generates the two trill types contain anatomically distinct populations of
482 neurons and are regulated independently.

483 In a variety of animals, generating different patterns of motor behaviors using the same
484 muscles is accomplished within the CNS in a number of different ways (such as biting and
485 chewing). First, related motor patterns can be generated by anatomically distinct networks
486 dedicated to each motor program (Huang and Satterlie 1990; Satterlie 2013). Second, they can
487 be generated by networks that are reorganized to be multifunctional (Berkowitz 2010; Dickinson
488 et al. 1990; Hooper and Moulins 1990; 1989; Li 2015; Meyrand et al. 1991; 1994; Popescu and
489 Frost 2002; Weimann and Marder 1994). A third strategy involves the combination of the two
490 (Berkowitz 2010; Briggman and Kristan 2006). Our results indicate that the circuits for fast trill
491 generators include a population of neurons in DTAM that are distinct from those involved in
492 slow trill generation, although the two circuits may share neurons in the n.IX-X. When the
493 projections between n.IX-X and DTAM are unilaterally transected in male *X. laevis*, fast trill
494 premotor activity recorded from DTAM became abnormal, and the fast trill (CAPs) recorded
495 from the transected side consistently lagged behind those recorded from the intact side while the
496 slow trill CAPs remained intact. These results are consistent with the idea that the transection
497 destroyed the core element of the fast trill rhythm generator on the transected side, while the fast
498 trill generator on the intact side and the slow trill generators on both sides remained intact. Thus,
499 we suggest that the fast trill CPG (labeled as green ovals with sinusoidal waves in Fig 8A)
500 includes a dedicated population of neurons (projection neurons that span n.IX-X and DTAM,
501 labeled with green double-arrows in Fig 8A) along with neurons in n.IX-X, whereas the slow trill

CPG consists of neurons in the n.IX-X (Fig 8A, labeled as blue circles with sinusoidal waves). Whether neurons in n.IX-X are shared by the two circuits is yet to be determined, but these are shown as separate populations in Fig 8A for simplicity.

Phylogenetically, males of the majority of the species in the genus *Xenopus* produce a series of sound pulses at rates similar to the fast trills of *X. laevis* while others produce sound pulses at a rate similar to or slower than the slow trills (Evans et al. 2015; Leininger et al. 2015; Tobias et al. 2011). It will be of interest to examine if all the species that generate fast trill-like calls utilize mechanisms that involves both nuclei whereas the slow trill-like calls are generated entirely by n.IX-X. Recent studies suggest that at least in two species of *Xenopus* that generate fast trill-like calls, DTAM premotor activity similar to that recorded in *X. laevis* is obtained (personal communication, Barkan CL, Zornik E, Kelley DB), supporting at least a part of this hypothesis. Additionally, we previously found that administration of androgen to adult females masculinizes them to produce male-like advertisement calls (Potter et al. 2005). As the vocalizations masculinize, it is possible that new projections between DTAM and n.IX-X are formed to construct the fast trill CPG *de novo*.

Fast and slow trill CPGs are contained in the two lateral hemispheres of the brainstem

A half-center hypothesis to explain mechanisms underlying rhythmic motor programs was originally proposed by Brown (Brown 1911; 1914), and has been examined both experimentally and computationally in a variety of species to date. Here, we asked whether the anterior and posterior commissures in the brainstem of *X. laevis* were components of a half-center oscillator, and are necessary for the production of fast and slow trill rhythms. Transection of the either one or both commissures did not result in the loss of fictive fast and slow trill

rhythms, except for a slight decrease in fictive fast trill rate, indicating that the commissures are not part of the half-center oscillators, and that the basic components of the fast and slow trill rhythm generators are contained in the two lateral halves of the brainstem. Although the sound pulse rates were largely unaffected, the vocalizations produced by the isolated hemi-brainstems were no longer bilaterally synchronized in brains in which both commissures were transected, indicating that the commissures function to synchronize the fast and slow trill generators on each side. Similar results were obtained in the Northern leopard frog; a complete sagittal bisection of the brainstem *in vitro* did not abolish fictive vocalizations elicited in response to electrical stimulation delivered to the anterior optic area (Schmidt 1992). In locomotor CPGs, surgical separation of the two sides of the spinal cord or pharmacological blockade of inhibitory synapses (including reciprocal inhibition) failed to abolish unilateral rhythmic activity underlying locomotor programs in lampreys, tadpoles, and mice (Cangiano and Grillner 2003; Cangiano et al. 2012; Cohen and Harris-Warrick 1984; Cowley and Schmidt 1995; Hinckley et al. 2005; Kwan et al. 2009; Li et al. 2010), suggesting that the commissures in the spinal cord of these species are not necessary components of the rhythm generating mechanisms. In contrast, locomotor CPGs of invertebrates have been shown to rely on half-center oscillators for rhythm generation (Sakurai et al. 2014; Satterlie 1985). Although these results seem to indicate that half-center oscillator play more dominant roles in invertebrates than in vertebrates, a recent study of a swimming CPG in *Xenopus* tadpoles showed that pharmacological blockade of reciprocal inhibition results in homeostatic change within the network that reinstate the rhythmic activity after tens of minutes (Moult et al. 2013). It is not clear how prevalent such homeostatic recovery is among different neural circuits, but it is possible that fictive fast and slow trill rhythms observed after >60 min of transection in this study may be due to *de novo* modification of the

neural circuits to regain function as in swimming circuits of *Xenopus* tadpoles. Future research that involves selective and fast inactivation of the commissural interneurons will be required to answer this question. At present, however, we tentatively conclude that there are fast and slow trill CPGs in each side of the brainstem (Fig 8A) that are coupled to each other via commissures.

Bilateral coordination of the two CPGs on the two lateral halves of the brainstem

Which projection neurons synchronize the fast and slow trill rhythms generated by the two CPGs in each half of the brainstem? We found that transection of the anterior commissure alone, the posterior commissure alone, and both commissures resulted in no delay (Fig 4), some delay (Fig 5), and no coordination (Fig 3) between the left and right CAPs, respectively. In addition, the loss of the posterior commissure sometimes resulted in asynchronous fictive slow trills from the two sides of the brainstem, whereas fictive fast trills never became asynchronous (Fig 5G). These results suggest that although the two commissures play a compensatory role in synchronizing the two CPGs on the both sides of the brainstem, the posterior commissure likely plays a more dominant role than the anterior commissure in coupling the two CPGs.

A previous anatomical study identified four types of commissural interneurons contained in the anterior and posterior commissures of the brainstem of *X. laevis*. The anterior commissure includes axons of DTAM neurons that project to the contralateral DTAM ($DTAM_{DTAM}$, Fig 8B) and of neurons that decussate first to the contralateral DTAM and project to the contralateral n.IX-X ($DTAM_{cn.IX\text{-}X}$, Fig 8B). The posterior commissure includes axons of n.IX-X neurons that project to the contralateral n.IX-X ($n.IX\text{-}X_{n.IX\text{-}X}$, Fig 8B) and the neurons that decussate to the contralateral n.IX-X and project to contralateral DTAM ($n.IX\text{-}X_{cDTAM}$, , Fig 8B, Zornik and Kelley 2007). Because the slow trill CPGs are likely contained in n.IX-X (Fig 8A), we propose

571 that projection neurons that terminate in n.IX-X (n.IX-$X_{n.IX-X}$ and $DTAM_{cn.IX-X}$) couple the two
572 slow trill CPGs (Fig 8A, blue arrows with filled arrowheads). Fast trill CPGs that span n.IX-X
573 and DTAM, in contrast, are proposed to be coupled by a population of neurons that terminate in
574 DTAM (n.IX-$X_{cn.DTAM}$ and $DTAM_{cDTAM}$, Fig 8A, green arrows with filled arrowheads).
575 Furthermore, we suggest, based on the degree of deterioration of bilateral synchrony observed
576 upon transections, that the coupling efficiency differs among these commissural interneurons.
577 The n.IX-$X_{cn.IX-X}$ and n.IX-$X_{cn.DTAM}$ axons contained in the posterior commissure likely couple
578 the rhythms generated by the fast and slow CPGs with maximum efficiency, because transection
579 of these axons resulted in significant delay or desynchronization between the two halves of the
580 fast and slow trill CPGs (Fig 8A, the coupling efficiency expressed as thick green and blue
581 arrows). $DTAM_{DTAM}$ and $DTAM_{cn.IX-X}$ axons contained in the anterior commissure couple the
582 fictive fast trill and slow trill rhythms with minimum efficiency because the loss of the anterior
583 commissure has little impact on the synchronous activity of the two nerves during the fictive fast
584 and slow trills (Fig 8A). In this model, the commissural interneurons that couple the CPGs on
585 the two sides synchronize the timing of the two oscillators by eliciting spikes from laryngeal
586 motor neurons from the right and left brainstem near simultaneously. The loss of these
587 commissural interneurons will result in either a delay between the rhythms generated by the two
588 oscillators (Fig 5E, F) or autonomous operation of each oscillator (Fig 5G).
589
590
591
592 **Mechanisms for fast and slow trill initiation and its bilateral synchronization**

In the present study, transections of the projections between extended amygdala and DTAM along with the anterior commissure revealed mechanisms underlying fast and slow trill initiation that appear to be distinct.

Slow trill initiation

Previously, we have shown that bilateral transection between n.IX-X and DTAM eliminates fictive advertisement calls entirely. If the projections between n.IX-X and DTAM are only necessary for the fast trill generation, but not for slow trill CPGs, why could we not elicit slow trills from any of the bilaterally transected brains? We suggest that there is a descending projection from DTAM to n.IX-X that *initiates* slow trill CPGs (Fig 8A, blue arrows with half-filled arrowheads); in the bilaterally transected brains, the signal to initiate the slow trill CPG is disrupted even though the CPG itself is intact. Interestingly, a slow trill almost always follows a fast trill, and is almost never produced in isolation both *in vivo* and *in vitro*. Thus, it is possible that the completion of the fast trill may generate a signal that descends from DTAM to n.IX-X to initiate slow trills. Regardless, we suggest that unilateral input from DTAM to n.IX-X is sufficient to initiate slow trills, as we have observed in unilaterally transected brains (Fig 2B), and the initiation of slow trills is bilaterally synchronized via anterior and posterior commissures (Fig 8A, blue lines with square ends). Accordingly, any transection in this study that left one of the two commissures intact (unilateral DTAM to n.IX-X transverse transection, anterior commissure sagittal transection, posterior commissure sagittal transection, descending transverse input together with anterior commissure sagittal transection) resulted in synchronized initiation of fictive slow trills (Fig 2B, 4B, 5B, 6B, F, H), whereas the transection that eliminated both

615 anterior and posterior commissure resulted in the autonomous initiation of fictive slow trills (Fig
616 3D, E).
617
618 *Fast trill initiation*
619 In brains in which both anterior and posterior commissures were transected, fictive fast
620 trills from the two isolated sides of the brainstems were initiated, on average, within 100
621 milliseconds of each other. The bath application technique used to apply 5-HT in the present
622 study does not necessarily activate the two DTAM simultaneously, because the patterns of
623 activation and desensitization of a population of receptors expressed by the two DTAMs are
624 different based on the geometric spread of the 5-HT solution through the recording chamber, or a
625 population of neurons downstream of the 5-HT signaling has different threshold for activation.
626 Thus, our results suggest the presence of a bilaterally synchronized descending signal from
627 extended amygdala that initiates fictive fast trills from the two sides of the brainstem within a
628 short time window (Fig 3E).
629 It was puzzling, however, that our previous study showed that the elimination of the
630 descending projections from extended amygdala to DTAM had no effect on the initiation of the
631 fictive fast trills in response to 5-HT (see Fig 7D, E, for example), while in this study we could
632 decouple the initiation of fast trills from the two sides of the brainstem by transecting both the
633 descending inputs to the brainstem and the anterior commissure. To explain these observations,
634 we propose that exogenous 5-HT initiates fictive fast trills in two complementary ways. One
635 way is to activate the extended amygdala, which sends bilateral descending signals to left and
636 right DTAM simultaneously, resulting in near synchronous activation of the fast trill CPG from
637 the two sides (Fig 8C, blue arrow). The other way is to activate a population of neurons in

638 DTAM unilaterally, which then project to contralateral DTAM via the anterior commissures and
639 result in simultaneous initiation of the fast trills from the two sides (Fig 8C, blue arrow). In the
640 latter scenario, we speculate that each DTAM is activated by 5-HT independently. Under this
641 scenario, unilateral activation of DTAM in brains without descending inputs (with intact anterior
642 commissures) can still initiate fictive advertisement calling by both halves of the brainstem via
643 the projection neurons connecting the two DTAMs through the anterior commissure (Fig 8A). In
644 brains with sagittal transection of anterior commissures (with intact descending inputs),
645 activation of the extended amygdala by 5-HT generates bilaterally synchronized initiation signals
646 which activate left and right DTAM to initiate advertisement calls from the two sides of the
647 brainstem simultaneously. It is only when both of these projections are removed that fast trills
648 are initiated by the left and right brainstem independently (Fig 8A).
649 Of these two projection neuron populations, however, the anterior commissure
650 projections appear to synchronize fictive fast trill onset more precisely than the bilateral
651 projections from the extended amygdala, because the initiation of DTAM activity in the absence
652 of anterior commissure (with or without posterior commissure) can result in a significant delay
653 between the two sides (Fig 3D, E, Fig 7J, L). Thus, we propose that the extended amygdala
654 signals that initiates fast trills from each side are permissive and allow fast trill initiations to take
655 place, but are not instructive in providing the timing information to initiate the fast trills.
656 Many episodic CPGs in vertebrates are considered to be initiated by the basal ganglia,
657 with its major function being to "select" appropriate behavior at any given moment (Hikosaka et
658 al., 1993, Mink 1996, Nambu et al., 2002). Vocal CPGs of a variety of vertebrate species are
659 also considered to be "selected" by the basal ganglia via periaqueductal gray (PAG, Hikosaka
660 2007). The vocal initiation mechanisms of *X. laevis*, however, may be distinct from other CPGs.

There has been no direct anatomical connections demonstrated between the PAG and the vocal nuclei, nor has there been any demonstration of the involvement of basal ganglia for vocal initiation to date in *X. laevis*. Instead, DTAM (also known as parabrachial area, Moreno and Gonzales 2005, Zornik and Kelley 2011 or pretrigeminal nucleus, Schmidt 1992) is reciprocally connected with the central amygdala (CeA), a nucleus included in extended amygdala, which is also reciprocally connected with PAG in *X. laevis* (Moreno and Gonzales 2005). The BNST, another nucleus included in the extended amygdala, directly projects to the dorsal raphe nucleus (Moreno et al. 2012), which sends serotonergic projections to n.IX-X and DTAM (Rhodes et al. 2007; Yu and Yamaguchi 2009; 2010). One study showed that lesion of CeA disrupts the production of vocal responses to females whereas lesioning of BNST decreases calling behavior *in vivo* in male *X. laevis* (Hall et al. 2013). This study suggests that CeA plays a role in eliciting vocalization in response to socially salient stimuli, whereas the BNST plays a role in initiating vocal activity in general. Previously, we have shown that increasing the extracellular concentration of endogenous serotonin using a selective serotonin reuptake inhibitor elicits fictive advertisement calls by activating 5-HT_{2C} receptors expressed in the raphe nucleus and n.IX-X (Yu and Yamaguchi 2010). Although transverse transection at the level of the rostral optic tectum did not allow us to identify which descending inputs play a role in initiating fast trills, we suggest that the BNST is a likely candidate nucleus that elicits fast trills from the brainstem.

Acknowledgements

We thank Matt Wachowiak and Erik Zornik, Paulo Rodrigues and two anonymous reviewers for helpful comments on this manuscript, and Malorie Jahn, Brandon Fisher, Shannon Roghaar, and Faith Denzer for analyzing data.

This work was supported by National Science Foundation 1146501, and startup funds provided by the Department of Biology and USTAR at the University of Utah (A.Y.).

Reference

Albersheim-Carter J, Blubaum A, Ballagh IH, Missaghi K, Siuda ER, McMurray G, Bass AH, Dubuc R, Kelley DB, Schmidt MF, Wilson RJ, and Gray PA. Testing the evolutionary conservation of vocal motoneurons in vertebrates. *Respir Physiol Neurobiol* 224: 2-10, 2016.

Bass AH, Gilland EH, and Baker R. Evolutionary origins for social vocalization in a vertebrate hindbrain-spinal compartment. *Science* 321: 417-421, 2008.

Berkowitz A. Multifunctional and specialized spinal interneurons for turtle limb movements. *Ann N Y Acad Sci* 1198: 119-132, 2010.

Briggman KL, and Kristan WB, Jr. Imaging dedicated and multifunctional neural circuits generating distinct behaviors. *J Neurosci* 26: 10925-10933, 2006.

Brown TG. The intrinsic factors in the act of progression in the mammal. *Proc R Soc Lond B* 84: 308-319, 1911.

Brown TG. On the nature of the fundamental activity of the nervous centres; together with an analysis of the conditioning of rhythmic activity in progression, and a theory of the evolution of function in the nervous system. *The Journal of physiology* 48: 18-46, 1914.

Buchanan JT. Flexibility in the patterning and control of axial locomotor networks in lamprey. *Integr Comp Biol* 51: 869-878, 2011.

Cangiano L, and Grillner S. Fast and slow locomotor burst generation in the hemispinal cord of the lamprey. *J Neurophysiol* 89: 2931-2942, 2003.

Cangiano L, Hill RH, and Grillner S. The hemisegmental locomotor network revisited. *Neuroscience* 210: 33-37, 2012.

Chagnaud BP, Baker R, and Bass AH. Vocalization frequency and duration are coded in separate hindbrain nuclei. *Nat Commun* 2: 346, 2011.

Cohen AH, and Harris-Warrick RM. Strychnine eliminates alternating motor output during fictive locomotion in the lamprey. *Brain Res* 293: 164-167, 1984.

Cowley KC, and Schmidt BJ. Effects of inhibitory amino acid antagonists on reciprocal inhibitory interactions during rhythmic motor activity in the in vitro neonatal rat spinal cord. *J Neurophysiol* 74: 1109-1117, 1995.

Dickinson PS, Mecsas C, and Marder E. Neuropeptide fusion of two motor-pattern generator circuits. *Nature* 344: 155-158, 1990.

Evans BJ, Carter TF, Greenbaum E, Gvozdik V, Kelley DB, McLaughlin PJ, Pauwels OS, Portik DM, Stanley EL, Tinsley RC, Tobias ML, and Blackburn DC. Genetics, Morphology, Advertisement Calls, and Historical Records Distinguish Six New Polyploid Species of African Clawed Frog (Xenopus, Pipidae) from West and Central Africa. *PLoS One* 10: e0142823, 2015.

Fetcho JR, and McLean DL. Some principles of organization of spinal neurons underlying locomotion in zebrafish and their implications. *Ann N Y Acad Sci* 1198: 94-104, 2010.

Garcia AJ, 3rd, Zanella S, Koch H, Doi A, and Ramirez JM. Chapter 3--networks within networks: the neuronal control of breathing. *Prog Brain Res* 188: 31-50, 2011.

Grillner S. Biological pattern generation: the cellular and computational logic of networks in motion. *Neuron* 52: 751-766, 2006.

Hall IC, Ballagh IH, and Kelley DB. The Xenopus amygdala mediates socially appropriate vocal communication signals. *J Neurosci* 33: 14534-14548, 2013.

Hinckley C, Seebach B, and Ziskind-Conhaim L. Distinct roles of glycinergic and GABAergic inhibition in coordinating locomotor-like rhythms in the neonatal mouse spinal cord. *Neuroscience* 131: 745-758, 2005.

Hooper SL, and Moulins M. Cellular and synaptic mechanisms responsible for a long-lasting restructuring of the lobster pyloric network. *J Neurophysiol* 64: 1574-1589, 1990.
Hooper SL, and Moulins M. Switching of a neuron from one network to another by sensory-induced changes in membrane properties. *Science* 244: 1587-1589, 1989.
Huang Z, and Satterlie RA. NEURONAL MECHANISMS UNDERLYING BEHAVIORAL SWITCHING IN A PTEROPOD MOLLUSC. *Journal of Comparative Physiology A Sensory Neural and Behavioral Physiology* 166: 875-888, 1990.
Jurgens U, and Hage SR. On the role of the reticular formation in vocal pattern generation. *Behav Brain Res* 182: 308-314, 2007.
Kiehn O, Dougherty KJ, Hagglund M, Borgius L, Talpalar A, and Restrepo CE. Probing spinal circuits controlling walking in mammals. *Biochem Biophys Res Commun* 396: 11-18, 2010.
Kwan AC, Dietz SB, Webb WW, and Harris-Warrick RM. Activity of Hb9 interneurons during fictive locomotion in mouse spinal cord. *J Neurosci* 29: 11601-11613, 2009.
Leininger EC, Kitayama K, and Kelley DB. Species-specific loss of sexual dimorphism in vocal effectors accompanies vocal simplification in African clawed frogs (Xenopus). *J Exp Biol* 218: 849-857, 2015.
Li WC. Selective Gating of Neuronal Activity by Intrinsic Properties in Distinct Motor Rhythms. *J Neurosci* 35: 9799-9810, 2015.
Li WC, Roberts A, and Soffe SR. Specific brainstem neurons switch each other into pacemaker mode to drive movement by activating NMDA receptors. *J Neurosci* 30: 16609-16620, 2010.
Marder E, and Bucher D. Central pattern generators and the control of rhythmic movements. *Curr Biol* 11: R986-996, 2001.
Marder E, Bucher D, Schulz DJ, and Taylor AL. Invertebrate central pattern generation moves along. *Curr Biol* 15: R685-699, 2005.
Marder E, and Calabrese RL. Principles of rhythmic motor pattern generation. *Physiol Rev* 76: 687-717, 1996.
Meyrand P, Simmers J, and Moulins M. Construction of a pattern-generating circuit with neurons of different networks. *Nature* 351: 60-63, 1991.
Meyrand P, Simmers J, and Moulins M. Dynamic construction of a neural network from multiple pattern generators in the lobster stomatogastric nervous system. *J Neurosci* 14: 630-644, 1994.
Moreno N, and Gonzalez A. Central amygdala in anuran amphibians: neurochemical organization and connectivity. *J Comp Neurol* 489: 69-91, 2005.
Moreno N, Morona R, Lopez JM, Dominguez L, Joven A, Bandin S, and Gonzalez A. Characterization of the bed nucleus of the stria terminalis in the forebrain of anuran amphibians. *J Comp Neurol* 520: 330-363, 2012.
Moult PR, Cottrell GA, and Li WC. Fast silencing reveals a lost role for reciprocal inhibition in locomotion. *Neuron* 77: 129-140, 2013.
Popescu IR, and Frost WN. Highly dissimilar behaviors mediated by a multifunctional network in the marine mollusk Tritonia diomedea. *J Neurosci* 22: 1985-1993, 2002.
Potter KA, Bose T, and Yamaguchi A. Androgen-induced vocal transformation in adult female African clawed frogs. *J Neurophysiol* 94: 415-428, 2005.
Rhodes HJ, Yu HJ, and Yamaguchi A. Xenopus vocalizations are controlled by a sexually differentiated hindbrain central pattern generator. *J Neurosci* 27: 1485-1497, 2007.
Roberts A, Li WC, and Soffe SR. A functional scaffold of CNS neurons for the vertebrates: the developing Xenopus laevis spinal cord. *Dev Neurobiol* 72: 575-584, 2012.

Sakurai A, Gunaratne CA, and Katz PS. Two interconnected kernels of reciprocally inhibitory interneurons underlie alternating left-right swim motor pattern generation in the mollusk Melibe leonina. *J Neurophysiol* 112: 1317-1328, 2014.
Satterlie RA. Reciprocal inhibition and postinhibitory rebound produce reverberation in a locomotor pattern generator. *Science* 229: 402-404, 1985.
Satterlie RA. Toward an organismal neurobiology: integrative neuroethology. *Integr Comp Biol* 53: 183-191, 2013.
Schmidt RS. Neural correlates of frog calling: production by two semi-independent generators. *Behav Brain Res* 50: 17-30, 1992.
Sweeney LB, and Kelley DB. Harnessing vocal patterns for social communication. *Curr Opin Neurobiol* 28: 34-41, 2014.
Tobias ML, Evans BJ, and Kelley DB. Evolution of advertisement calls in African clawed frogs. *Behaviour* 148: 519-549, 2011.
Weimann JM, and Marder E. Switching neurons are integral members of multiple oscillatory networks. *Curr Biol* 4: 896-902, 1994.
Yager DD. A unique sound production mechanism in the pipid anuran Xenopus borealis. *Zoological Journal of the Linnean Society* 104: 351-375, 1992.
Yamaguchi A, and Kelley DB. Generating sexually differentiated vocal patterns: laryngeal nerve and EMG recordings from vocalizing male and female african clawed frogs (Xenopus laevis). *J Neurosci* 20: 1559-1567, 2000.
Yu HJ, and Yamaguchi A. 5-HT2C-like receptors in the brain of Xenopus laevis initiate sex-typical fictive vocalizations. *J Neurophysiol* 102: 752-765, 2009.
Yu HJ, and Yamaguchi A. Endogenous serotonin acts on 5-HT2C-like receptors in key vocal areas of the brain stem to initiate vocalizations in Xenopus laevis. *J Neurophysiol* 103: 648-658, 2010.
Zornik E, Katzen AW, Rhodes HJ, and Yamaguchi A. NMDAR-dependent control of call duration in Xenopus laevis. *J Neurophysiol* 103: 3501-3515, 2010.
Zornik EJ. Regulating breathing and calling in an aquatic frog : neuronal networks in the Xenopus laevis hindbrain. 2007.

Figure Captions

Figure 1. Advertisement calls generated by male *Xenopus laevis*. A. Simultaneous recordings of the sound (top trace) and the laryngeal nerve activity (lower trace) while advertisement calls are produced by an awake male *Xenopus laevis*. Fast trills are enveloped in green, slow trills in blue. A sound pulse (black arrowheads, top trace) is always preceded by a compound action potential (gray arrowheads, bottom trace). B. Diagram of the key vocal nuclei of male *Xenopus laevis*. Within a brainstem, a pair of dorsal tegmental area of medulla (DTAM) and a pair of laryngeal motor nuclei (n.IX-X) are contained. These nuclei are reciprocally connected with each other by projection neurons (solid arrows). DTAMs, in turn, are reciprocally connected with the extended amygdala (EA). A pair of extended amygdala are reciprocally connected, but the coupling is shown as a line in the diagram, since we did not explore the function of bilateral coupling of EA in this study.

Figure 2. Effects of unilateral, transverse transection of projections between DTAM and n.IX-X. A. Diagram of the vocal pathways with transection marked with a red line with scissors, disconnected projections in dotted arrows, and intact projections in solid black arrows. B. DTAM local field potential (LFP, top and bottom traces) and laryngeal nerve recordings (middle two traces) obtained from right and left DTAMs and nerves while a fictive advertisement call is generated by an isolated brain, before transection. Green and blue frames indicate fast and slow trills, respectively. C. Fast and slow trill rates before and after transection. Each pair of points indicates mean fast and slow trill rates before and after the transection in one animal. Pairs of dotted green and blue lines indicate the range of fast and

853 slow trill rates obtained from intact brains. D. Enlarged sections of brackets labeled in B. Left
854 (blue traces) and right (red traces) nerve recordings are shown during fast and slow trills with
855 the overlay of the two nerves at the bottom. E. Example of cross correlation between left and
856 right nerve recordings (see Methods) for fast and slow trills before and after transection. Each
857 line represent cross correlation of a bout of fast or slow trills from one animal (cross correlation
858 of ten bouts shown). F. Absolute peak lag time before and after the transection for fast and
859 slow trills, plotted for each animal as in (C). Asterisk, significant difference ($p < 0.05$); n.s., not
860 significant. G. Mean CAP amplitude during fast and slow trills obtained from brains before
861 and after the transection. Each pair of points indicates mean fast and slow trill CAP amplitude
862 before and after the transection in one animal. H. Example power spectra of the DTAM LFP
863 recordings during fast trills from both sides of DTAM before and after transection. Black
864 arrow on the bottom right graph ('Post-transection Right DTAM') indicates the loss of peak at
865 60Hz after the transection.
866
867 Figure 3. Effects of sagittal transection of both anterior and posterior commissures on fictive
868 vocalizations. A. Diagram of the vocal pathways showing transections in red lines with
869 scissors, transected projections in dotted arrows, and intact projections in solid arrows. B.
870 Example bilateral DTAM local field potential (LFP) recordings (top and bottom traces) and
871 laryngeal nerve recordings (middle two traces) obtained during fictive advertisement calls
872 before transection. Green and blue frames indicate fast and slow trills, respectively, for all
873 figures. Rectangle shows transition from slow trills to fast trills. C. Enlarged sections of
874 brackets labeled in (B). Left (blue traces) and right (red traces) nerve recordings are shown
875 during fast and slow trills with the overlay of nerve activities at the bottom. D. Example

bilateral DTAM LFP and laryngeal nerve recordings obtained from a brain in which both anterior and posterior commissures are sagitally transected. Bracket with black arrow in the bottom trace points to a fictive advertisement call produced only by the right nerve. E. Enlarged sections from small brackets labeled in (D). F. Example of cross correlation between left and right nerve recordings for fast and slow trills before (intact) and after transection (post-transection). There is no obvious peak in correlation coefficient after the transection, indicating the asynchronous nature of the two nerve activities. G. Mean fast and slow trill rates before and after transection from three brains. Because asynchronous fictive calls were recorded from the right and left nerve, the trill rates from the two sides were analyzed as independent rhythms after transection. Points connected by a line indicates mean fast and slow rate of one animal. Pairs of dotted green and blue lines indicate the range of fast and slow trill rates obtained from intact brains. Asterisk, significant difference ($p<0.05$); n.s., not significant. H. Example of fictive advertisement calls recorded from the right and left laryngeal nerves from brains with both anterior and posterior commissures sagitally transected. Note that the left and right calls are largely overlapping, but slow trills are sometimes missing on one nerve (black arrows).

Figure 4. Effects of sagitally transecting anterior commissure alone on fictive advertisement calls. A. Diagram of the vocal pathways showing the transection in red line with scissors, transected projections in dotted arrows, and intact projections in solid arrows. B. Example bilateral DTAM LFP (top and bottom traces) and laryngeal nerve recordings (middle two traces) obtained during a fictive advertisement call from a brain after anterior commissure sagittal transection. Green and blue frames indicate fast and slow trills, respectively. C. Mean fast and slow trill rates before and after transection from six brains. Points connected by a line

indicates mean fast and slow rate of one animal. Pairs of dotted green and blue lines indicate the range of fast and slow trill rates obtained from intact brains. D. Enlarged sections of brackets labeled in B. Left (blue traces) and right (red traces) nerve recordings are shown during fast and slow trills with the overlay of the two nerve activity at the bottom. E. Example of cross correlation between the left and right nerve recordings for fast and slow trills before and after transection. F. Absolute peak lag time before and after transection, plotted for each animal as in (C). n.s., not significant difference.

Figure 5. Effects of sagitally transecting the posterior commissure alone on fictive advertisement calls. A. Diagram of the vocal pathways showing the transection in red line with scissors, transected projections in dotted arrows, and intact projections in solid arrows. B. Example bilateral DTAM LFP and laryngeal nerve recordings obtained during fictive advertisement call after posterior commissure sagittal transection. Green and blue frames indicate fast and slow trills, respectively, for all figures. C. Mean fast and slow trill rates before and after transection from six brains. Each pair of points indicates mean rate before and after transection in one animal. Pairs of dotted green and blue lines indicate the range of fast and slow trill rates obtained from intact brains. D. Enlarged sections of brackets labeled in (B). Left (blue traces) and right (red traces) nerve recordings are shown during fast and slow trills with the overlay of the nerve activities at the bottom. E. Example cross correlation between the left and right nerve recordings for fast and slow trills before and after transection. F. Absolute peak lag time before and after the transection, plotted for each animal as in (C). Asterisks indicate statistically significant differences ($p<0.05$). G. Example left and right

nerve recordings during a fictive fast and slow trill. In this recording, left and right CAPs are largely asynchronous only during the slow trill.

Figure 6. Effects of simultaneously eliminating the anterior commissure and the projection between the extended amygdala and DTAM on fast trill initiation. A. Diagram of the vocal pathways showing the transection in red line with scissors, transected projections in dotted arrows, and intact projections in solid arrows. B. Example bilateral DTAM LFP (top and bottom traces) and nerve recordings (middle two traces) obtained from double-transected brains. Dark and light green frames indicate the side with the larger and smaller amplitude fast trill CAPs, respectively. Blue frames indicate slow trills. During Fast Trill 1 and 3,CAPs are larger on the right nerve than the left nerve, and during Fast Trill 2 and 4, CAPs are larger on the left nerve than the right nerve. Black arrows indicate the unilateral absence of the DTAM activity. C. Mean fast and slow trill rates before and after transection. Each pair of points indicates mean trill rates for one animal. Pairs of dotted green and blue lines indicate the range of fast and slow trill rates obtained from intact brains. D, E. Enlarged views of the brackets labeled in (B). D1, E1. Example of cross correlation between the left and right nerve shown in (D) and (E). Here, the cross correlation coefficient was calculated by sliding recording of a single CAP obtained from one nerve against the other nerve (as opposed to using nerve recordings of a whole fast trills, as done in previous figures). Peak cross correlation coefficient at negative or positive lag time indicates left nerve leading right or right nerve leading left, respectively. F. Example bilateral DTAM LFP (top and bottom traces) and laryngeal nerve recordings (middle two traces) during which both left and right DTAM becomes active. Dark and light green frames indicate the side with larger and smaller amplitude fast trill CAPs, respectively, as in (B).

944 Blue frame indicates a slow trill. G. Enlarged view of the bracket labeled in (F). Left (blue
945 trace) and right (red trace) nerve recordings are shown with the overlay of the nerve activities at
946 the bottom. Blue and red straight lines under the traces indicate the time during which left and
947 right DTAM is active, respectively. G1. Example of cross correlation between the left and
948 right nerve. Note that the peak cross correlation coefficients are distributed among positive and
949 negative lag times, indicating CAPs recorded from one nerve do not consistently lead those
950 recorded from the other nerve. H. Example bilateral nerve recordings obtained from double-
951 transected brains that include slow trills. I. Enlarged view of the bracket labeled in (H). I1.
952 Example of cross correlation between the left and right nerves during slow trills. Note that
953 peak cross correlation coefficients are centered at zero, indicating that the CAPs recorded from
954 the two nerves are synchronous.
955
956 Figure 7. Effects of transecting the projection between extended amygdala and DTAM alone,
957 or the anterior commissure alone, on the initiation of DTAM premotor activity and fast trills. A.
958 Example bilateral DTAM LFP (top and bottom traces) and nerve recordings (middle two traces)
959 obtained from an intact brain. Green and blue frames indicate fast and slow trills, respectively,
960 for all figures. B. Enlarged view of the bracket labeled in (A). The first premotor activity
961 recorded from left and right DTAM is labeled with large black arrows (top and bottom traces),
962 and the first fast trill CAPs recorded from the left and right nerves are labeled with a small
963 double-headed arrow between the two middle traces. Note that both DTAM activity and CAPs
964 are initiated simultaneously from the left and right. C, F. Diagram showing transection site in
965 red line with scissors, transected projections in dotted arrows, and intact projections in solid
966 arrows. D, G, I, K. Example bilateral DTAM LFP (top and bottom traces) and nerve

recordings (middle two traces) obtained after transection to eliminate the projections between extended amygdala and DTAM (D) or anterior commissure (G, I, K). E, H, J, L. Enlarged view of the bracket labeled in (D, G, I, K). The first premotor activity recorded from left and right DTAM is labeled with large black arrows on top and bottom traces, and the first fast trill CAPs recorded from the left and right nerves are labeled with a double-headed arrows between the middle two traces, as in (B). Note that DTAM premotor activity starts simultaneously in E and H, but not in J and L. The first fast trill CAPs, in contrast, are always recorded simultaneously from the two nerves in these transected brains.

Figure 8. Model of the vocal CPGs in male *Xenopus laevis*. A. Functional model of the central vocal pathways of male *Xenopus laevis*. Green oval and blue circle containing sinusoidal waveform indicate central pattern generators for fast and slow trills, respectively. B. Four different types of anatomically identified projection neurons in the central vocal pathways of *Xenopus laevis*. Axons of these neurons are contained in anterior or posterior commissures. C: Solid blue arrows indicate hypothesized redundant mechanisms of vocal initiation by serotonin (5-HT).

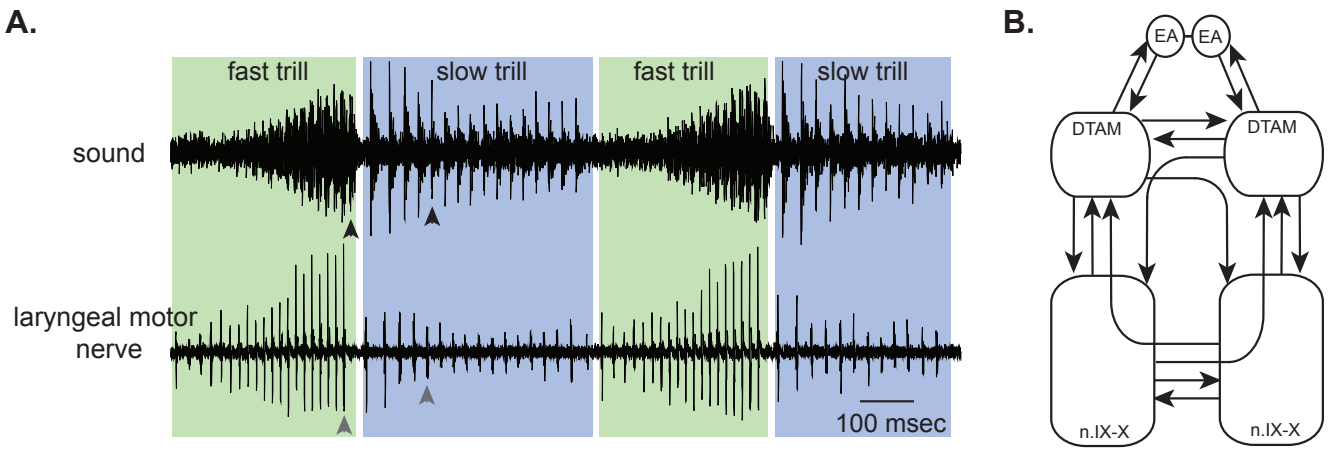
A.
fast trill
slow trill
fast trill
slow trill
sound
laryngeal motor nerve
100 msec
B.
EA
EA
DTAM
DTAM
n.IX-X
n.IX-X

Figure 1

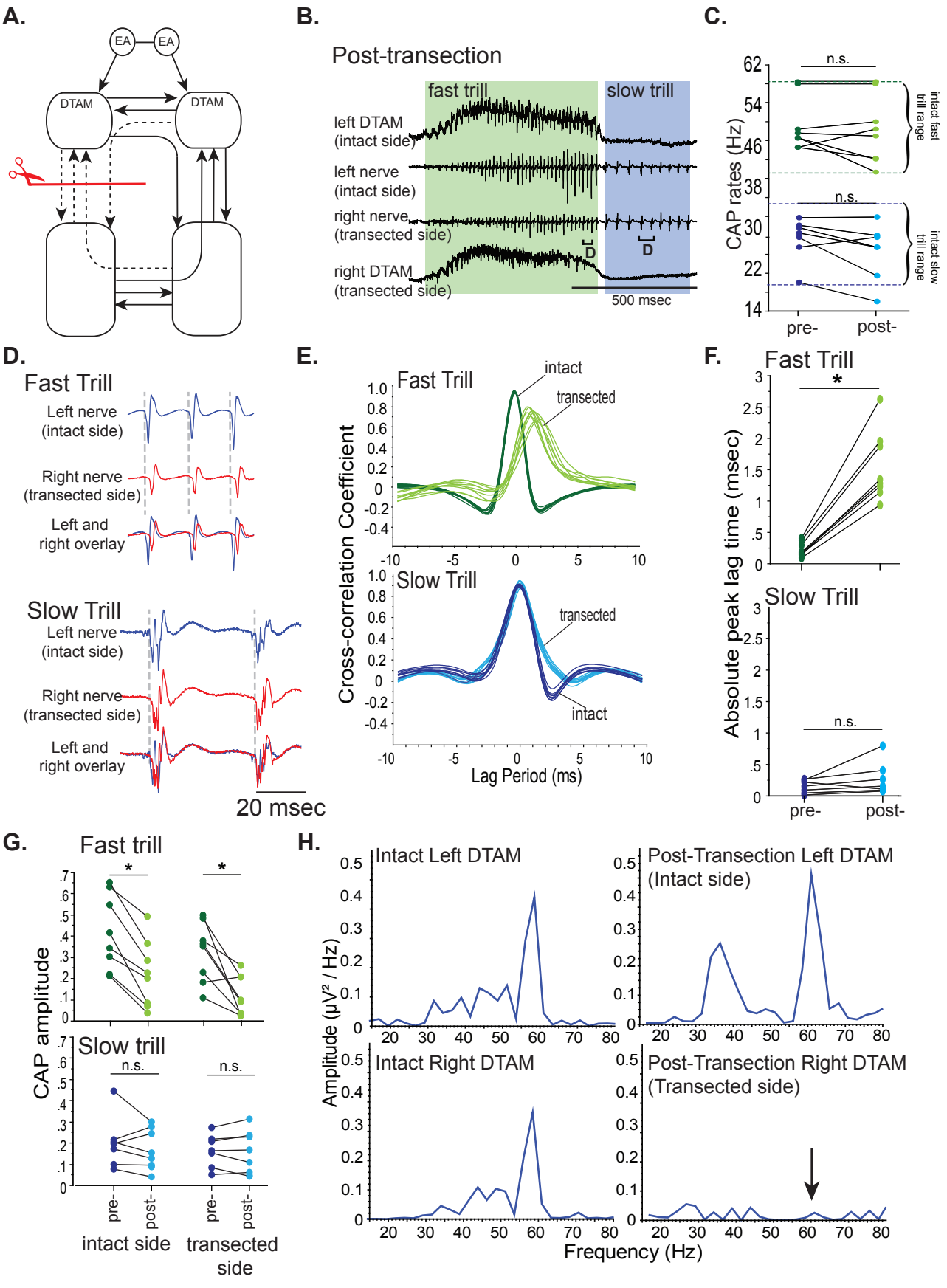
A.
EA
EA
DTAM
DTAM
B.
Post-transection
fast trill
slow trill
left DTAM
(intact side)
left nerve
(intact side)
right nerve
(transected side)
right DTAM
(transected side)
500 msec
C.
n.s.
n.s.
intact fast trill range
intact slow trill range
CAP rates (Hz)
62
54
46
38
30
22
14
pre-
post-
D.
Fast Trill
Left nerve
(intact side)
Right nerve
(transected side)
Left and
right overlay
Slow Trill
Left nerve
(intact side)
Right nerve
(transected side)
Left and
right overlay
20 msec
E.
Fast Trill
intact
transected
Slow Trill
transected
intact
Cross-correlation Coefficient
Lag Period (ms)
F.
Fast Trill
Slow Trill
Absolute peak lag time (msec)
n.s.
pre-
post-
G.
Fast trill
Slow trill
CAP amplitude
n.s.
n.s.
pre-
post-
pre-
post-
intact side
transected
side
H.
Intact Left DTAM
Post-Transection Left DTAM
(Intact side)
Intact Right DTAM
Post-Transection Right DTAM
(Transected side)
Amplitude (μV² / Hz)
Frequency (Hz)

Figure 2

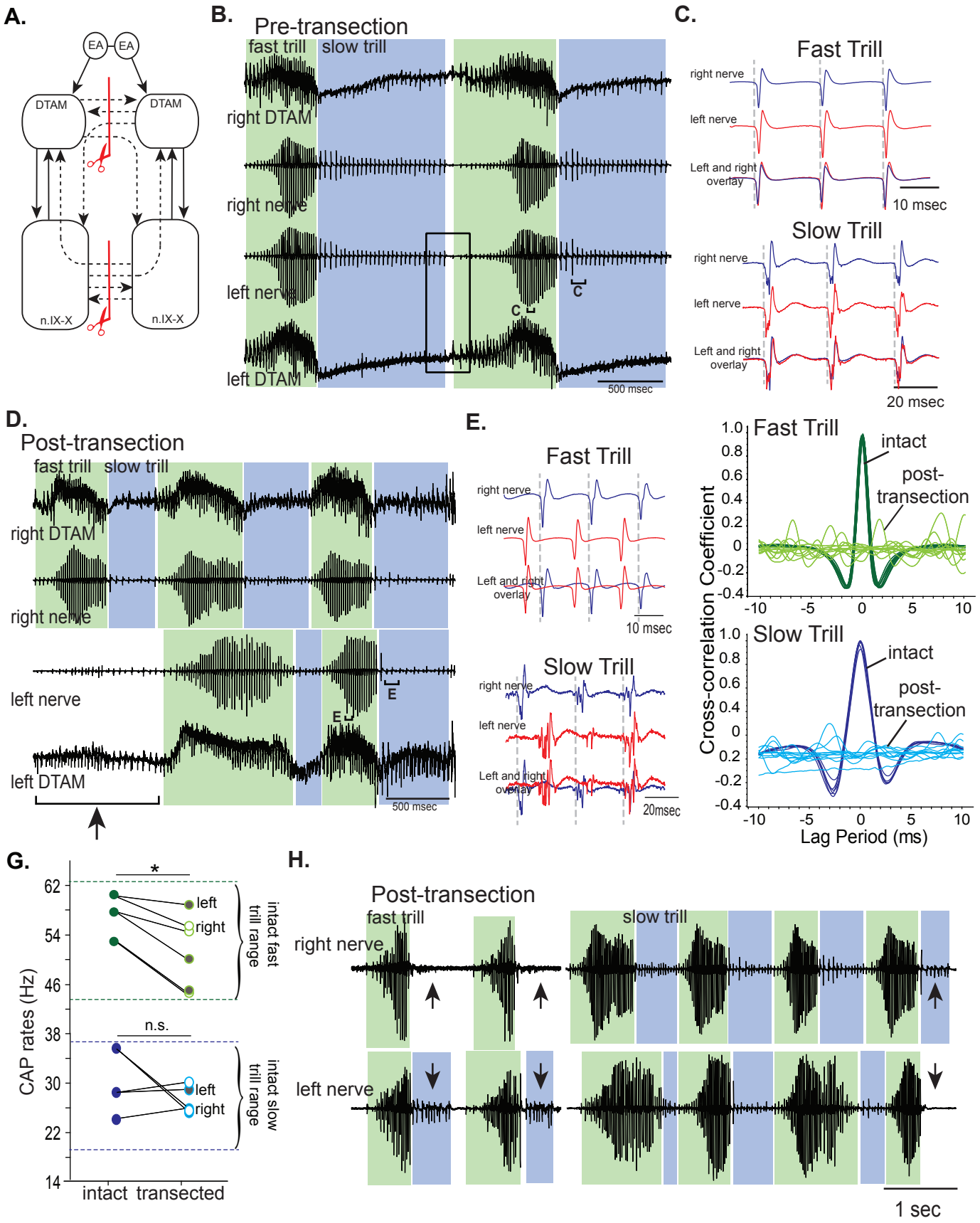
A.
EA
EA
DTAM
DTAM
n.IX-X
n.IX-X
B.
Pre-transection
fast trill
slow trill
right DTAM
right nerve
left nerve
left DTAM
C
C
500 msec
C.
Fast Trill
right nerve
left nerve
Left and right overlay
10 msec
Slow Trill
right nerve
left nerve
Left and right overlay
20 msec
D.
Post-transection
fast trill
slow trill
right DTAM
right nerve
left nerve
left DTAM
E
E
500 msec
E.
Fast Trill
right nerve
left nerve
Left and right overlay
10 msec
Slow Trill
right nerve
left nerve
Left and right overlay
20msec
Fast Trill
intact
post-transection
Slow Trill
intact
post-transection
Cross-correlation Coefficient
1.0
0.8
0.6
0.4
0.2
0
-0.2
-0.4
-10
-5
0
5
10
Lag Period (ms)
G.
*
n.s.
left
right
left
right
intact fast trill range
intact slow trill range
CAP rates (Hz)
62
54
46
38
30
22
14
intact
transected
H.
Post-transection
fast trill
slow trill
right nerve
left nerve
1 sec

Figure 3

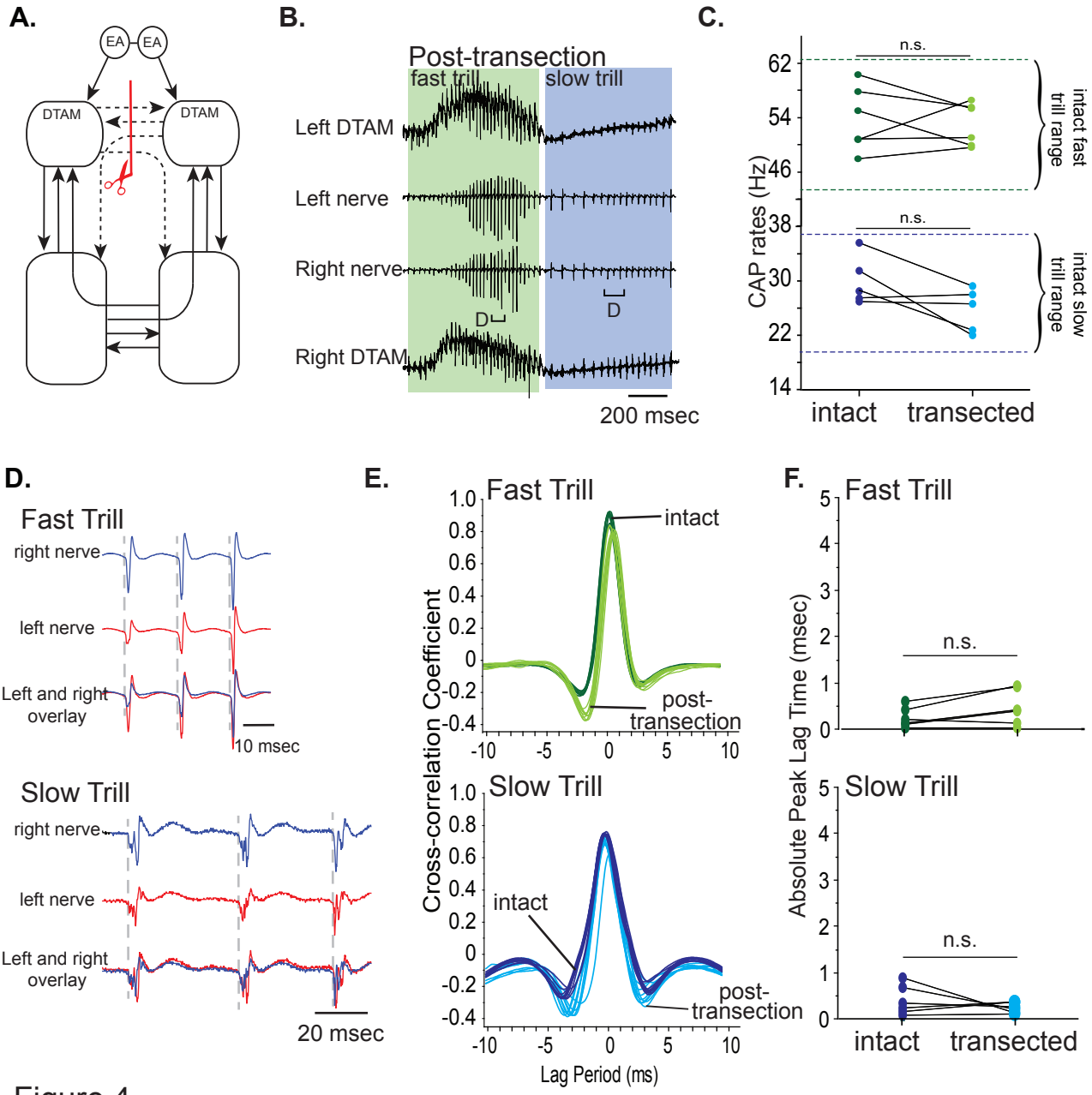
A.
EA
EA
DTAM
DTAM
B.
Post-transection
fast trill
slow trill
Left DTAM
Left nerve
Right nerve
Right DTAM
D
D
200 msec
C.
n.s.
n.s.
62
54
46
38
30
22
14
CAP rates (Hz)
intact fast trill range
intact slow trill range
intact
transected
D.
Fast Trill
right nerve
left nerve
Left and right overlay
10 msec
Slow Trill
right nerve
left nerve
Left and right overlay
20 msec
E.
Fast Trill
intact
post-transection
Slow Trill
intact
post-transection
Cross-correlation Coefficient
Lag Period (ms)
F.
Fast Trill
n.s.
Slow Trill
n.s.
Absolute Peak Lag Time (msec)
intact
transected

Figure 4

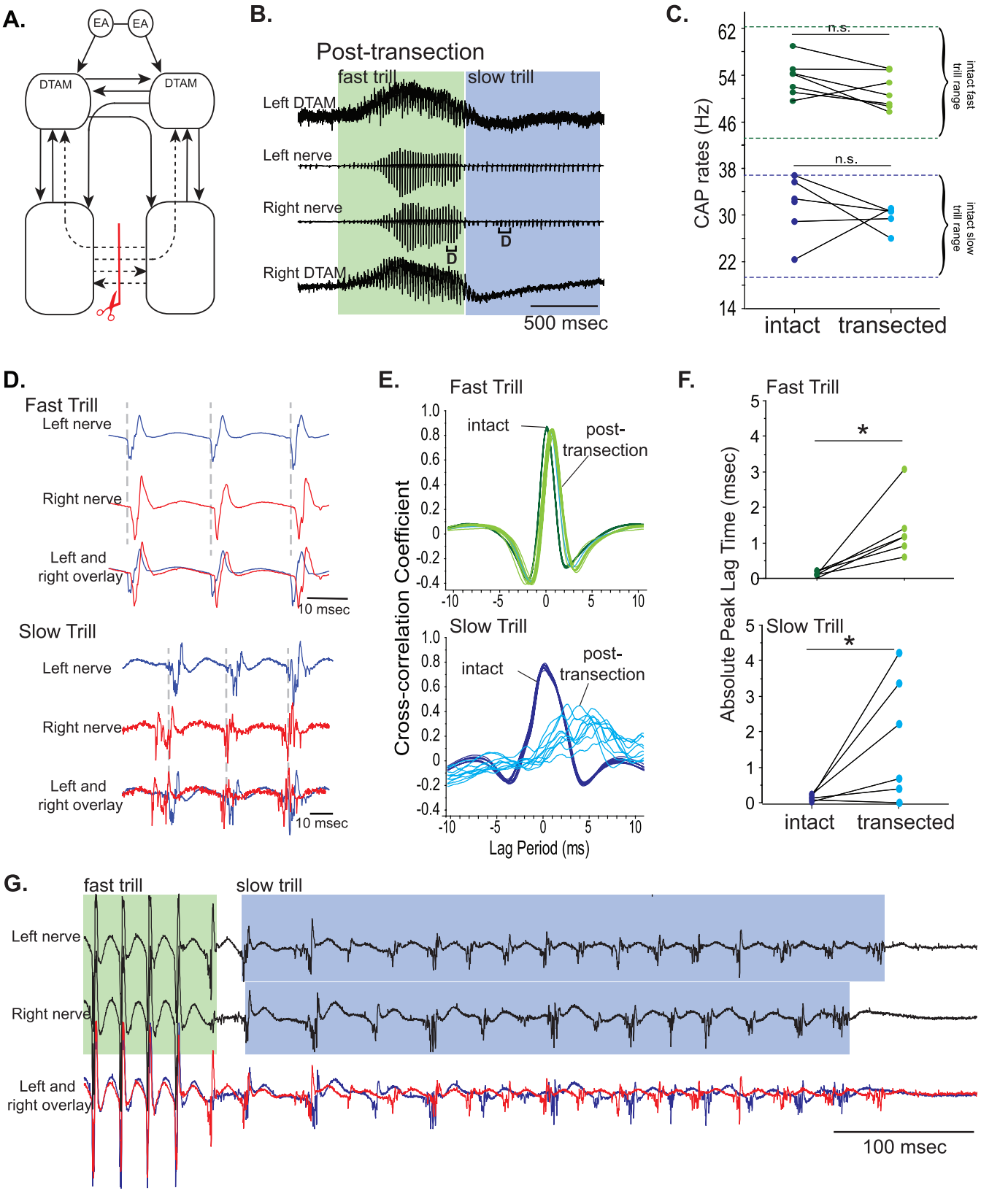
A.
EA
EA
DTAM
DTAM
B.
Post-transection
fast trill
slow trill
Left DTAM
Left nerve
Right nerve
Right DTAM
D
D
500 msec
C.
CAP rates (Hz)
62
54
46
38
30
22
14
n.s.
n.s.
intact fast trill range
intact slow trill range
intact
transected
D.
Fast Trill
Left nerve
Right nerve
Left and right overlay
10 msec
Slow Trill
Left nerve
Right nerve
Left and right overlay
10 msec
E.
Fast Trill
intact
post-transection
Slow Trill
intact
post-transection
Cross-correlation Coefficient
1.0
0.8
0.6
0.4
0.2
0
-0.2
-0.4
-10
-5
0
5
10
Lag Period (ms)
F.
Fast Trill
Slow Trill
Absolute Peak Lag Time (msec)
5
4
3
2
1
0
*
*
intact
transected
G.
fast trill
slow trill
Left nerve
Right nerve
Left and right overlay
100 msec

Figure 5

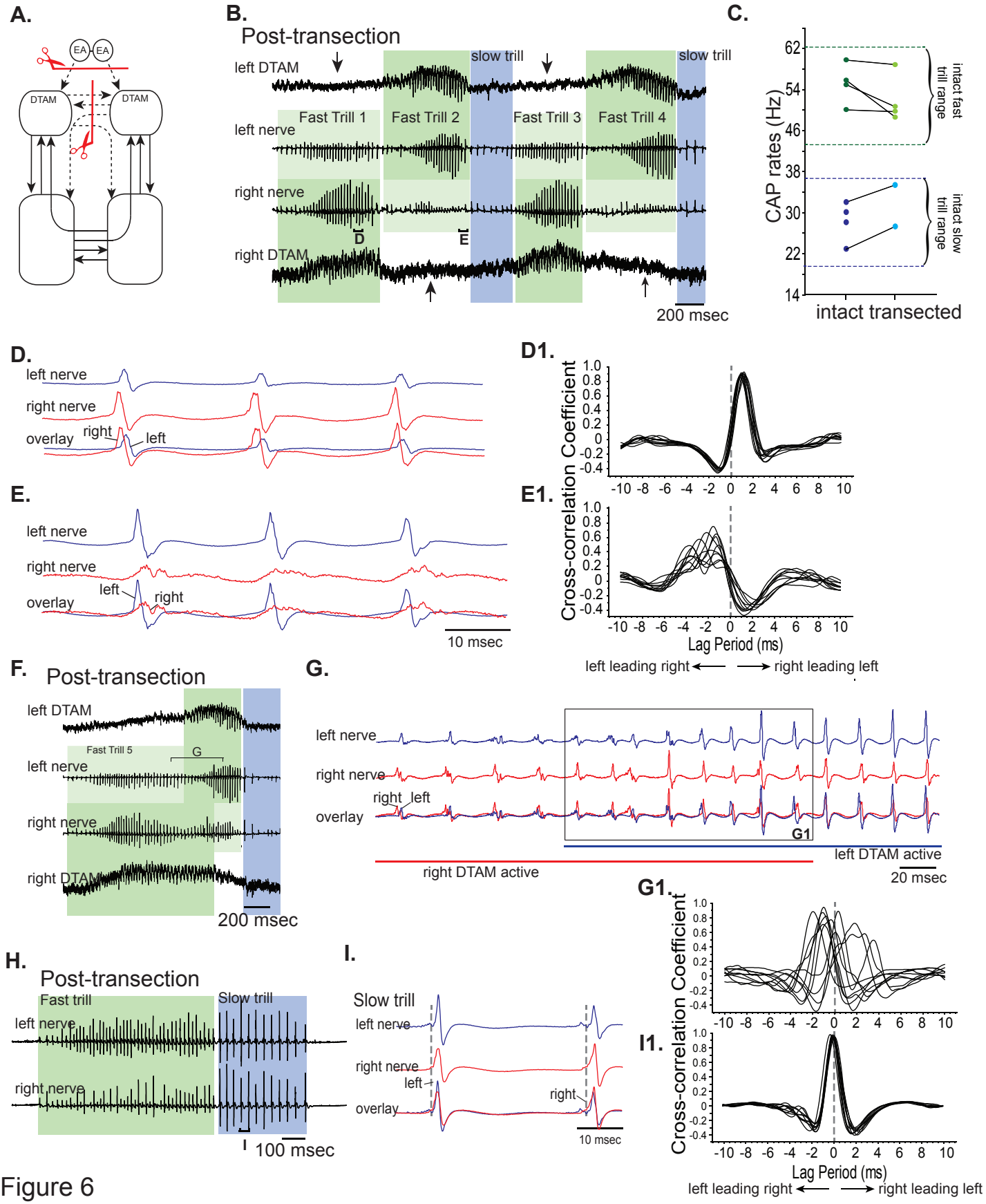
A.
EA
EA
DTAM
DTAM
B.
Post-transection
left DTAM
slow trill
slow trill
Fast Trill 1
Fast Trill 2
Fast Trill 3
Fast Trill 4
left nerve
right nerve
D
E
right DTAM
200 msec
C.
CAP rates (Hz)
62
54
46
38
30
22
14
intact fast trill range
intact slow trill range
intact transected
D.
left nerve
right nerve
overlay
right
left
D1.
Cross-correlation Coefficient
1.0
0.8
0.6
0.4
0.2
0
-0.2
-0.4
-10 -8 -6 -4 -2 0 2 4 6 8 10
E.
left nerve
right nerve
overlay
left
right
10 msec
E1.
Cross-correlation Coefficient
Lag Period (ms)
left leading right
right leading left
F.
Post-transection
left DTAM
Fast Trill 5
G
left nerve
right nerve
right DTAM
200 msec
G.
left nerve
right nerve
right
left
overlay
G1
left DTAM active
right DTAM active
20 msec
G1.
Cross-correlation Coefficient
H.
Post-transection
Fast trill
Slow trill
left nerve
right nerve
100 msec
I.
Slow trill
left nerve
right nerve
left
right
overlay
10 msec
I1.
Cross-correlation Coefficient
Lag Period (ms)
left leading right
right leading left

Figure 6

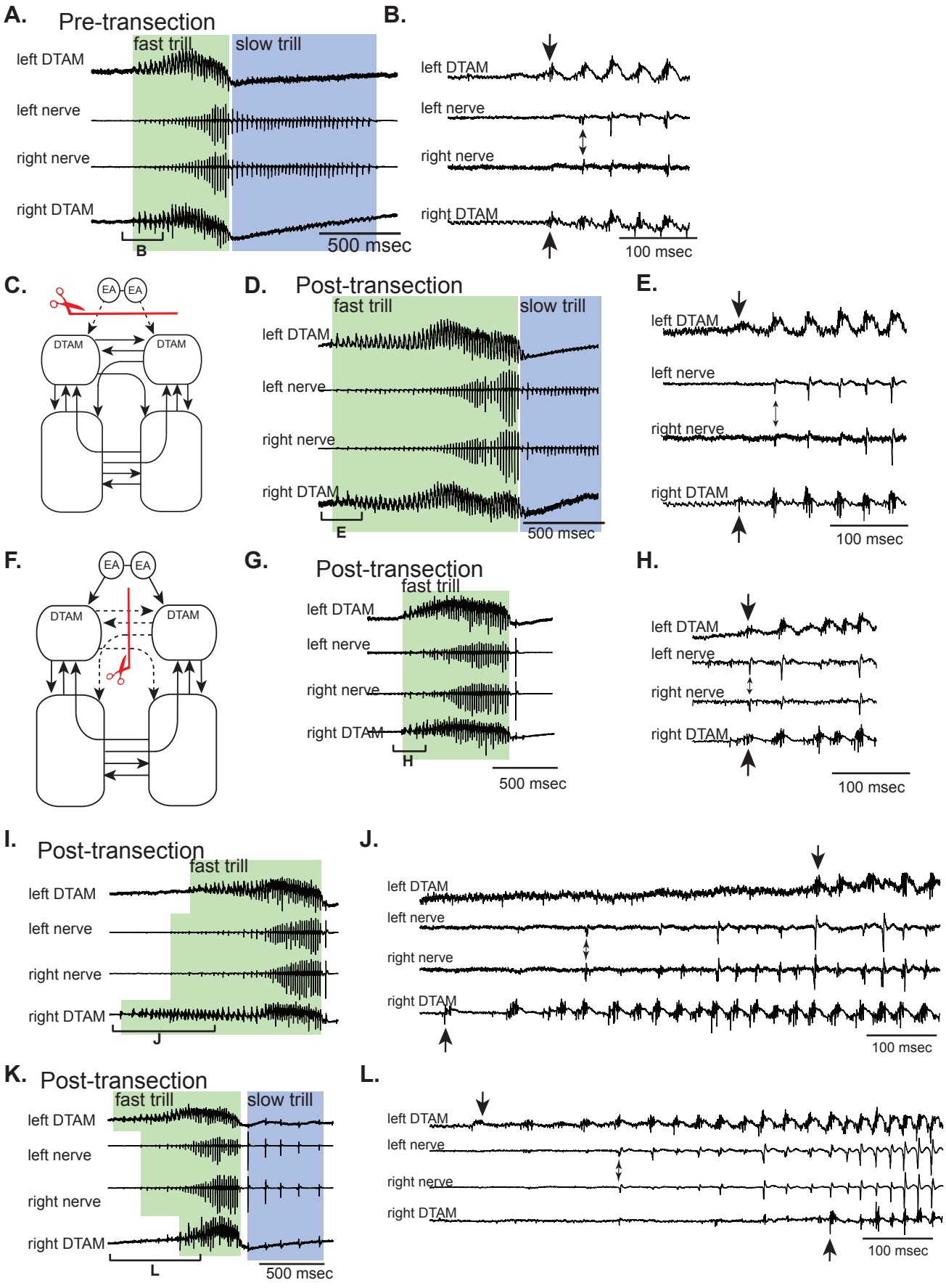
A.
Pre-transection
fast trill
slow trill
left DTAM
left nerve
right nerve
right DTAM
B
500 msec
B.
left DTAM
left nerve
right nerve
right DTAM
100 msec
C.
EA
EA
DTAM
DTAM
D.
Post-transection
fast trill
slow trill
left DTAM
left nerve
right nerve
right DTAM
E
500 msec
E.
left DTAM
left nerve
right nerve
right DTAM
100 msec
F.
EA
EA
DTAM
DTAM
G.
Post-transection
fast trill
left DTAM
left nerve
right nerve
right DTAM
H
500 msec
H.
left DTAM
left nerve
right nerve
right DTAM
100 msec
I.
Post-transection
fast trill
left DTAM
left nerve
right nerve
right DTAM
J
J.
left DTAM
left nerve
right nerve
right DTAM
100 msec
K.
Post-transection
fast trill
slow trill
left DTAM
left nerve
right nerve
right DTAM
L
500 msec
L.
left DTAM
left nerve
right nerve
right DTAM
100 msec

Figure 7

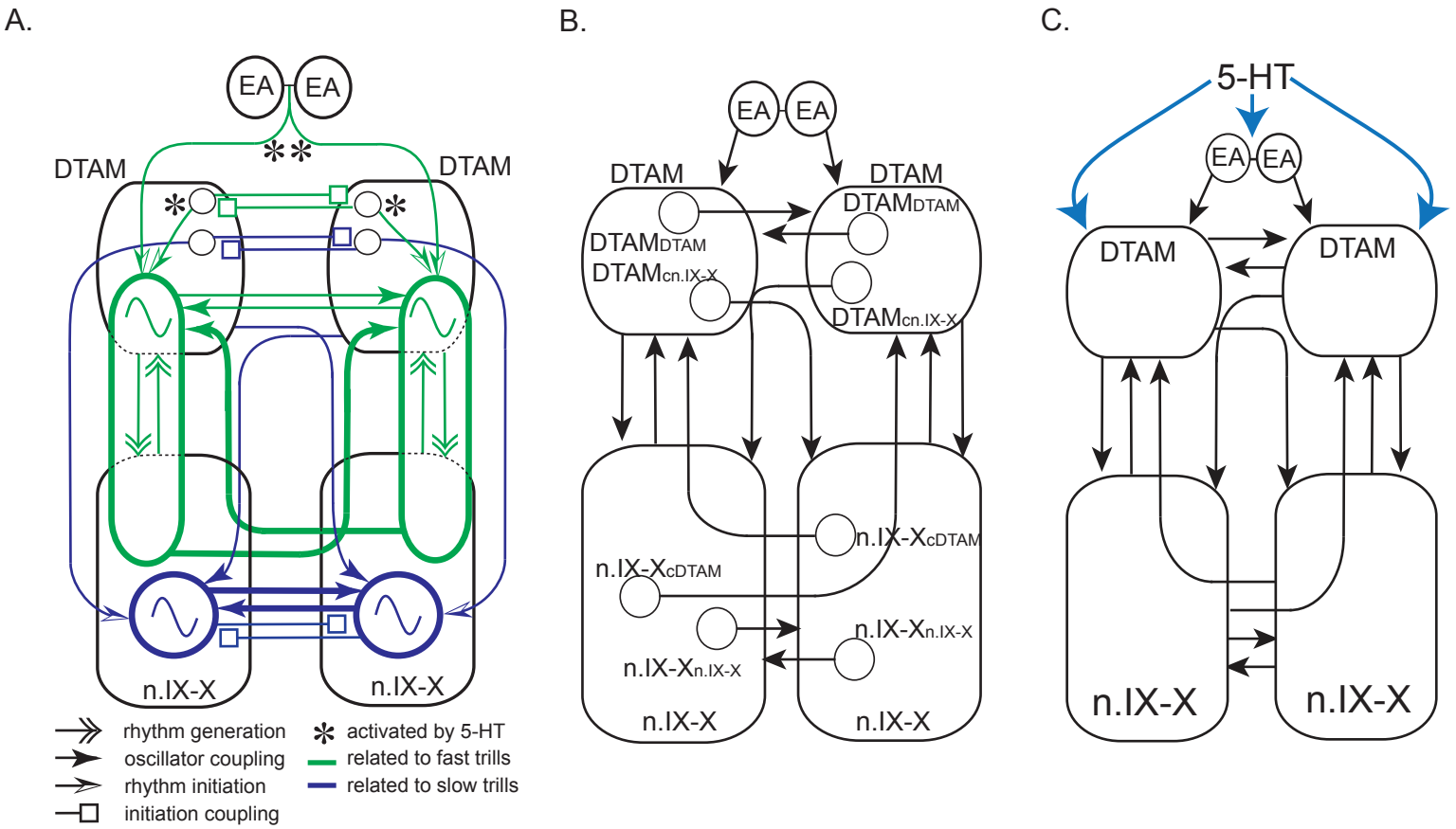
A.
EA
EA
DTAM
DTAM
n.IX-X
n.IX-X
rhythm generation
oscillator coupling
rhythm initiation
initiation coupling
activated by 5-HT
related to fast trills
related to slow trills
B.
EA
EA
DTAM
DTAM
DTAMDTAM
DTAMcn.IX-X
DTAMDTAM
DTAMcn.IX-X
n.IX-XcDTAM
n.IX-XcDTAM
n.IX-Xn.IX-X
n.IX-Xn.IX-X
n.IX-X
n.IX-X
C.
5-HT
EA
EA
DTAM
DTAM
n.IX-X
n.IX-X

Figure 8